

Aberystwyth University

Ice-dammed lateral lake and epishelf lake insights into Holocene dynamics of Margeurite Trough Ice Stream and George VI Ice Shelf, Alexander Island, Antarctic Peninsula

Davies, Bethan Joan; Hambrey, Michael; Glasser, Neil; Holt, Thomas; Rodés, Angél; Smellie, John L.; Carrivick, Jonathan L.; Blockley, Simon P. E.

Published in:
Quaternary Science Reviews

DOI:
[10.1016/j.quascirev.2017.10.016](https://doi.org/10.1016/j.quascirev.2017.10.016)

Publication date:
2017

Citation for published version (APA):
Davies, B. J., Hambrey, M., Glasser, N., Holt, T., Rodés, A., Smellie, J. L., Carrivick, J. L., & Blockley, S. P. E. (2017). Ice-dammed lateral lake and epishelf lake insights into Holocene dynamics of Margeurite Trough Ice Stream and George VI Ice Shelf, Alexander Island, Antarctic Peninsula. *Quaternary Science Reviews*, 177, 189-219. <https://doi.org/10.1016/j.quascirev.2017.10.016>

Document License CC BY

General rights

Copyright and moral rights for the publications made accessible in the Aberystwyth Research Portal (the Institutional Repository) are retained by the authors and/or other copyright owners and it is a condition of accessing publications that users recognise and abide by the legal requirements associated with these rights.

- Users may download and print one copy of any publication from the Aberystwyth Research Portal for the purpose of private study or research.
- You may not further distribute the material or use it for any profit-making activity or commercial gain
- You may freely distribute the URL identifying the publication in the Aberystwyth Research Portal

Take down policy

If you believe that this document breaches copyright please contact us providing details, and we will remove access to the work immediately and investigate your claim.

tel: +44 1970 62 2400
email: is@aber.ac.uk



Ice-dammed lateral lake and epishelf lake insights into Holocene dynamics of Marguerite Trough Ice Stream and George VI Ice Shelf, Alexander Island, Antarctic Peninsula

Bethan J. Davies^{a, b, *}, Michael J. Hambrey^b, Neil F. Glasser^b, Tom Holt^b, Angél Rodés^c, John L. Smellie^d, Jonathan L. Carrivick^e, Simon P.E. Blockley^a

^a Centre for Quaternary Research, Royal Holloway University of London, Egham, Surrey, TW20 0EX, UK

^b Institute of Geography and Earth Sciences, Aberystwyth University, Ceredigion, SY23 3DB, Wales, UK

^c SUERC, Rankine Avenue, East Kilbride, G75 0QF, Scotland, UK

^d Department of Geology, University of Leicester, Leicester, LE1 7RH, UK

^e School of Geography and Water@leeds, University of Leeds, Woodhouse Lane, Leeds, West Yorkshire, LS2 9JT, UK

ARTICLE INFO

Article history:

Received 5 June 2017

Received in revised form

1 October 2017

Accepted 12 October 2017

Keywords:

Holocene

George VI Ice Shelf

Marguerite Trough Ice Stream

Antarctica

Cosmogenic isotope dating

Geomorphology

ABSTRACT

We present new data regarding the past dynamics of Marguerite Trough Ice Stream, George VI Ice Shelf and valley glaciers from Ablation Point Massif on Alexander Island, Antarctic Peninsula. This ice-free oasis preserves a geological record of ice stream lateral moraines, ice-dammed lakes, ice-shelf moraines and valley glacier moraines, which we dated using cosmogenic nuclide ages. We provide one of the first detailed sediment-landform assemblage descriptions of epishelf lake shorelines. Marguerite Trough Ice Stream imprinted lateral moraines against eastern Alexander Island at 120 m at Ablation Point Massif. During deglaciation, lateral lakes formed in the Ablation and Moutonnée valleys, dammed against the ice stream in George VI Sound. Exposure ages from boulders on these shorelines yielded ages of 13.9 to 9.7 ka. Following recession of the ice stream, George VI Ice Shelf formed in George VI Sound. An epishelf lake formed at 15–20 m asl in Ablation and Moutonnée valleys, dated from 9.4 to 4.6 ka, suggesting that the lake was stable and persistent for some 5000 years. Lake-level lowering occurred after this, with the lake level at 12 m at 3.1 ± 0.4 ka and at 5 m asl today. A readvance of the valley glaciers on Alexander Island at 4.4 ± 0.7 ka is recorded by valley glacier moraines overlying epishelf lake sediments. We speculate that the glacier readvance, which occurred during a period of warmth, may have been caused by a dynamic response of the glaciers to a lowering in surface elevation of George VI Ice Shelf.

© 2017 The Authors. Published by Elsevier Ltd. This is an open access article under the CC BY license (<http://creativecommons.org/licenses/by/4.0/>).

1. Introduction

Alexander Island, western Antarctic Peninsula, is a region that has had limited terrestrial glaciological research but has potential to yield insights into a variety of important processes. The Antarctic Peninsula is currently warming rapidly, which has resulted in ice-sheet thinning (Pritchard and Vaughan, 2007) and the dramatic collapse of several ice shelves (Cook and Vaughan, 2010), some of which have maintained stable grounding lines for millennia (Rebesco et al., 2014). These collapse events have been followed by accelerated flow of grounded ice (De Angelis and Skvarca, 2003;

Scambos et al., 2004; Berthier et al., 2012) and glacier recession (Glasser et al., 2011; Davies et al., 2012). Quantifying the timing and environmental conditions surrounding Holocene ice-shelf collapse events is therefore particularly pertinent to assessing future ice-shelf stability and the threat of collapse. Reconstructing past rates, volumes and magnitudes of ice sheet, ice shelf and glacier change, and their response to changing oceanic and climatic regimes, is vital in providing a context for this change, to improve predictions of future ice-sheet behaviour (Bentley, 2010), and to provide glacial-isostatic adjustment corrections for gravimetric measurements of contemporary ice loss (King et al., 2012). The terrestrial record of Holocene valley glacier fluctuations at the large ice-free oases at Ablation Point Massif on Alexander Island have the potential to provide a sensitive proxy climatic record, and is particularly important because Holocene glacier fluctuations are

* Corresponding author. Centre for Quaternary Research, Royal Holloway University of London, Egham, Surrey, TW20 0EX, UK.

E-mail address: Bethan.davies@rhul.ac.uk (B.J. Davies).

poorly understood across the Antarctic Peninsula (Carrivick et al., 2012; Ó Cofaigh et al., 2014). George VI Sound has been identified as a particularly important place for better constraints on past sea level, ice sheet, ice shelf and glacier change, yet rates of relative sea level change and isostatic uplift (Whitehouse et al., 2012b) and the timing of glacier and ice-shelf interaction and recession are poorly resolved here.

Ablation Point Massif bears a rare record of epishelf lake fluctuations. Epishelf lakes form when a floating ice shelf blocks the mouth of a fjord or valley, and they maintain a direct hydraulic connection to the sea under the base of the ice shelf. Meltwater flows from the ice shelf into the lake and is impounded behind the ice shelf. As freshwater is less dense than sea water, the freshwater floats on top of marine waters in a layer that is as deep as the ice shelf. The sediment-landform assemblage associated with epishelf lake sediments has received little attention in the literature (cf. Hendy et al., 2000; Hall et al., 2006). Much of the literature focuses on the ice-covered lakes in the Dry Valleys, which, although not epishelf lakes, have similar processes (e.g., Doran et al., 2000). However, awareness of the importance of these sediments in places such as the Arctic as well as in the Antarctic is growing (e.g., Van Hove et al., 2001; England et al., 2009; Antoniadou et al., 2011; Hamilton et al., 2017). Detailed descriptions of palaeo epishelf lake shorelines are therefore required in order to facilitate their recognition elsewhere in the landscape.

The aim of this paper is to determine ice sheet, valley glacier and ice shelf interactions during the Holocene Epoch in George VI Sound and on Alexander Island, western Antarctic Peninsula, an area with a well preserved but poorly dated terrestrial record (Sugden and Clapperton, 1981; Clapperton and Sugden, 1982, 1983; Roberts et al., 2008). We characterise sediment-landform assemblages and develop landform models to reconstruct Holocene valley glacier fluctuations and their relationship with former ice-shelf collapse events. We use cosmogenic nuclide dating from overlapping valley glacier moraines, epishelf lake shorelines and ice-shelf moraines to create the first regional reconstruction of Holocene valley glacier fluctuations. We link these data to local epishelf lake sediment data (Smith et al., 2007a; Roberts et al., 2008) and marine records of Holocene ice-shelf behaviour (e.g. Ó Cofaigh et al., 2005a). Moreover, we evaluate sediment/landform associations, and determine and date palaeo shorelines and ice-shelf moraines at a range of altitudes using cosmogenic nuclide dating. In this paper, we present 15 new ^{10}Be cosmogenic nuclide exposure ages and geomorphological mapping undertaken in November to December 2012 from lake shorelines, ice shelf moraines and valley glacier moraines around Ablation Point Massif, Alexander Island (Fig. 1).

2. Background to the research

2.1. Geographical and geological context

Alexander Island (68°S to 72°S; Fig. 1) is a largely ice-covered island that lies west of Palmer Land on the Antarctic Peninsula. It is separated from the Antarctic Peninsula by George VI Sound, which is ~500 km long, 25–70 km wide, and 400–1000 m deep (Bishop and Walton, 1981). The steep-sided trough extends northwards beyond the ice shelf and across the continental shelf of Marguerite Bay, and was occupied by Marguerite Trough Ice Stream during the Last Glacial Maximum (LGM) (Ó Cofaigh et al., 2005a; Jamieson et al., 2012). The island is 430 km long from its northernmost to southernmost point, covers 48,300 km² and has peaks rising as nunataks to 2500 m in the north of the island, whilst the southernmost parts of the island reach >500 m asl. A spine of high ground running north-south down the axis of the island forms the

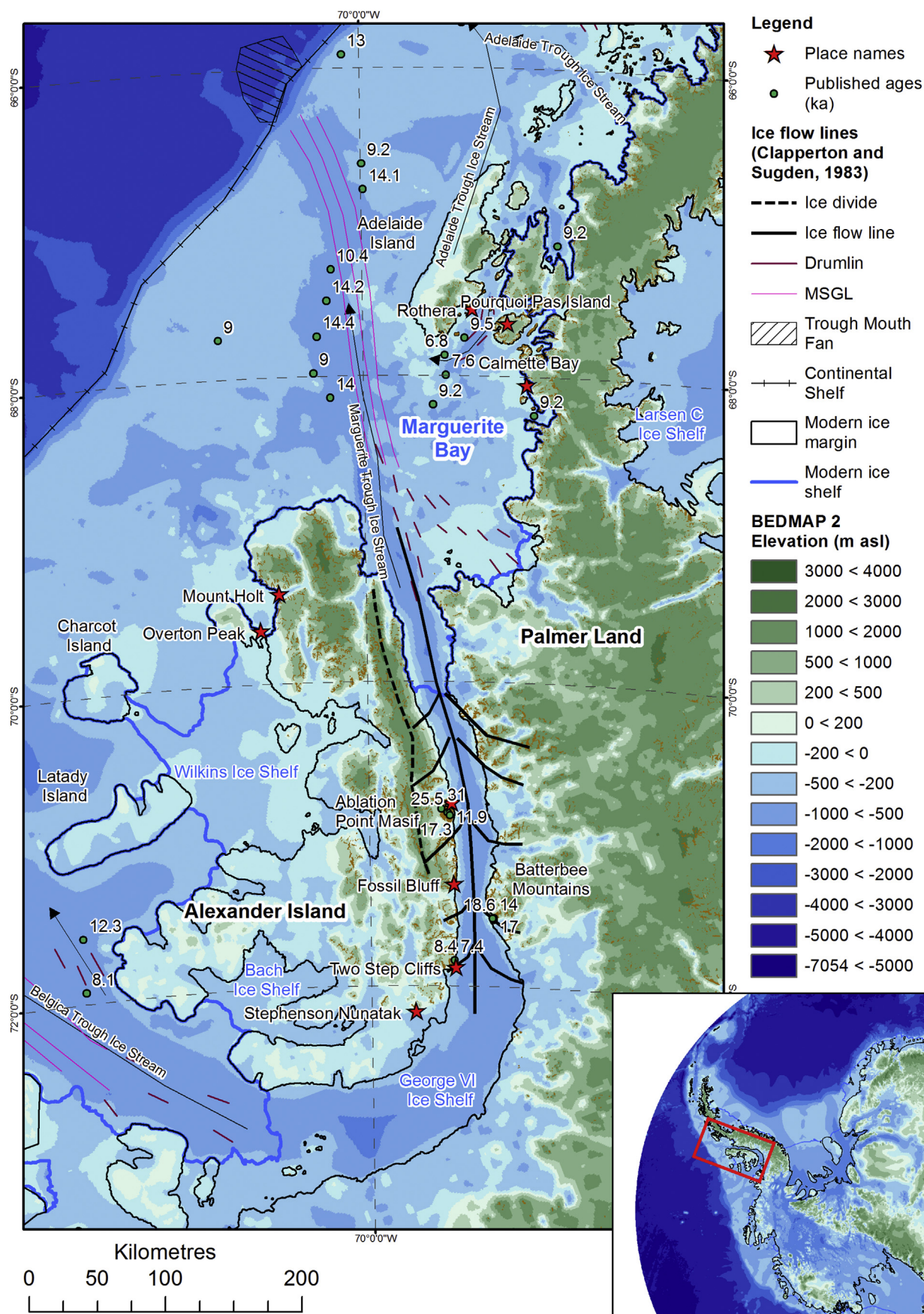
contemporary ice divide. There are several large ice-free areas at sea level on the eastern coast of Alexander Island: Ablation Point Massif (70°49'S, 68°15'W), Fossil Bluff (71°19'S, 68°21'W) and Two Steps Cliffs (71°53'S, 68°19') (Fig. 1).

Alexander Island has a mean annual air temperature of c. –9 °C (Morris and Vaughan, 2003). Fossil Bluff experienced mean summer and winter temperatures of –1.9 °C and –17.9 °C, respectively, between 1961 and 1994. Summer months with average temperatures above freezing were rare over this time period, though mean summer temperatures have been increasing at +0.4 °C per decade (Harangozo et al., 1997). Precipitation data for Ablation Point Massif and Fossil Bluff have not been measured but Heywood (1977) assume from measured net accumulation on a glacier that mean annual precipitation is less than 0.20 m w.e. per year. Stephenson Nunatak, 100 km south of Fossil Bluff and also on eastern Alexander Island (Fig. 1), had a mean annual accumulation rate of 0.7 ± 0.2 m w.e. per year over the period 1986–1989 (Morris and Mulvaney, 1996; Morris, 1999). However, values of up to 2 m w.e. per year could occur on the northern spine and mountains of Alexander Island (Turner et al., 2002; van Lipzig et al., 2004). The snow largely ablates away during the summer season, leaving bare glacier ice and ground (Rau et al., 2000). The eastern and south-eastern parts of the island are drier (van Lipzig et al., 2004), following depletion of the moisture of the predominant westerlies (Turner et al., 2002), which accounts for the low-altitude ice-free oases on eastern Alexander Island. Fossil Bluff and Ablation Point Massif, on the drier eastern part of the island, therefore experience a continental, rather than maritime, climate, with low precipitation and low mean annual air temperatures (Harangozo et al., 1997).

Western Palmer Land is primarily composed of gabbro, white granite with pods of amphibolite, gneiss, granodiorite and tonalite from the Late Cretaceous to Early Tertiary Antarctic Peninsula Batholith (Fig. 2) (Leat et al., 1995). Volcanic outcrops are also present and comprise the Cretaceous, mainly basalt–andesite, Antarctic Peninsula Volcanic Group and the Jurassic, mainly dacite–rhyolite, Palmer Land Volcanic Group (formerly Ellsworth Land Volcanic Group; Smith, 1987; Hunter et al., 2006; Smellie, 2017). In contrast, eastern Alexander Island comprises the Jurassic to Cretaceous Fossil Bluff Group, with shale, sandstone, siltstone, mudstone, chert, greywacke and conglomerate (Fig. 2) (Butterworth et al., 1988). The Alexander Island conglomerates contain fluvially transported plutonic pebbles (0.5–30 cm), which are easily distinguished from Palmer Land granites by their well-rounded nature and darker petrographic composition (Roberts et al., 2008). The Fossil Bluff Group is bounded to the west by deformed subduction complex metasediments of the LeMay Group (Burn, 1984). Finally, volcanic rocks of the Alexander Island Volcanic Group, with mainly basalt–andesite compositions, occupy a linear belt on the west flank of the LeMay Range (McCarron and Smellie, 1998).

2.2. George VI Ice Shelf

George VI Ice Shelf (GVIIS) presently occupies George VI Sound. The long-term stability of George VI Ice Shelf is a critical question, as this may help us to assess its potential for future collapse. This ice shelf covers approximately 24,000 km² and is the second largest ice shelf remaining on the west Antarctic Peninsula (Holt et al., 2013). The northern ice front (~20 km wide) calves into Marguerite Bay, and the southern ice front (~75 km wide) terminates into the Ronne Entrance and is interrupted by ice rises on the Eklund Islands and De Atley Island (Fig. 1). The centreline distance between these two ice fronts is ~450 km (Holt et al., 2013). The ice-shelf catchment covers much of the eastern coast of Alexander Island and the western coast of Palmer Land (Fig. 2). Tributary glaciers from



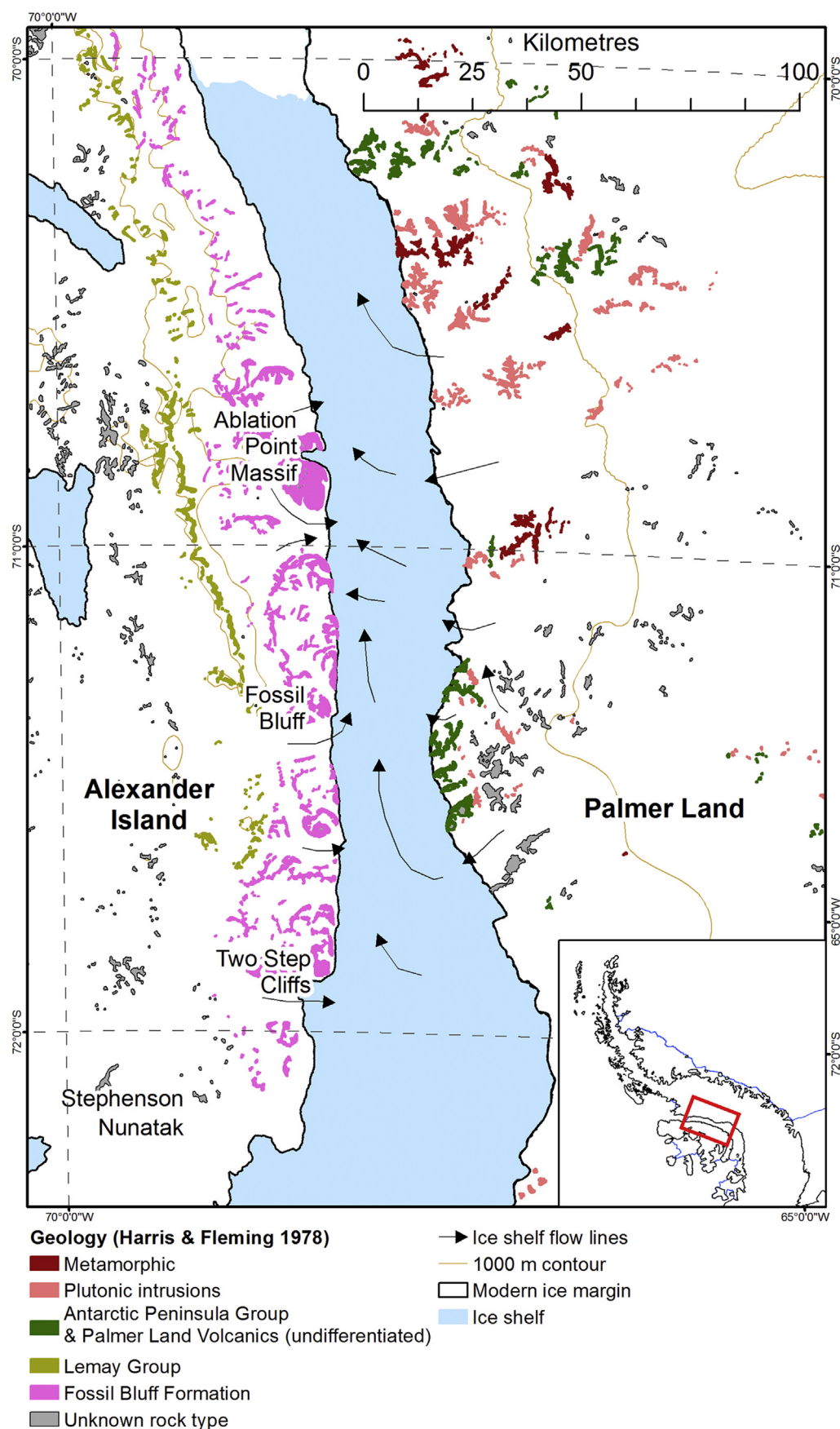


Fig. 2. Geological map showing ice-shelf flow lines and published geology (after Harris and Fleming, 1978; Reynolds and Hambrey, 1988). George VI Ice Shelf is shown in blue. (For interpretation of the references to colour in this figure legend, the reader is referred to the web version of this article.)

Alexander Island are much smaller (54–144 km²) and extend only a few kilometres into the ice-shelf system (Reynolds and Hambrey, 1988; Humbert, 2007).

The freeboard (height of the ice-shelf surface above sea level) of GVIS ranges from ~60 to 5 m asl (Fig. 3A). The ice shelf is structurally complex, with distinct flow units originating in Palmer Land flowing across to, and impinging against, Alexander Island (Reynolds and Hambrey, 1988; Hambrey et al., 2015). Ice-shelf thickness and freeboard is controlled by this complex flow regime. Ice-shelf thickness varies from 100 m at the northern ice front to 600 m in the centre, before thinning again towards the

southern ice front (Lucchitta and Rosanova, 1998; Smith et al., 2007a) (Fig. 3B). The thickest ice occurs in lobes extending from the grounding-lines of the major outlet glaciers from Palmer Land. Thicknesses adjacent to Ablation Point Massif are c. 125 m (Hambrey et al., 2015), and the ice-shelf surface is 5 m asl here. In the centre of George VI Sound near Ablation Point Massif, the ice shelf reaches up to 150 m thick (Fig. 3B). The ice shelf reaches a surface elevation of ~20 m asl at Fossil Bluff, with a thickness of ~200 m.

GVIS is of interest because it is near the −9 °C mean annual isotherm, which has been proposed as the limit of viability of ice

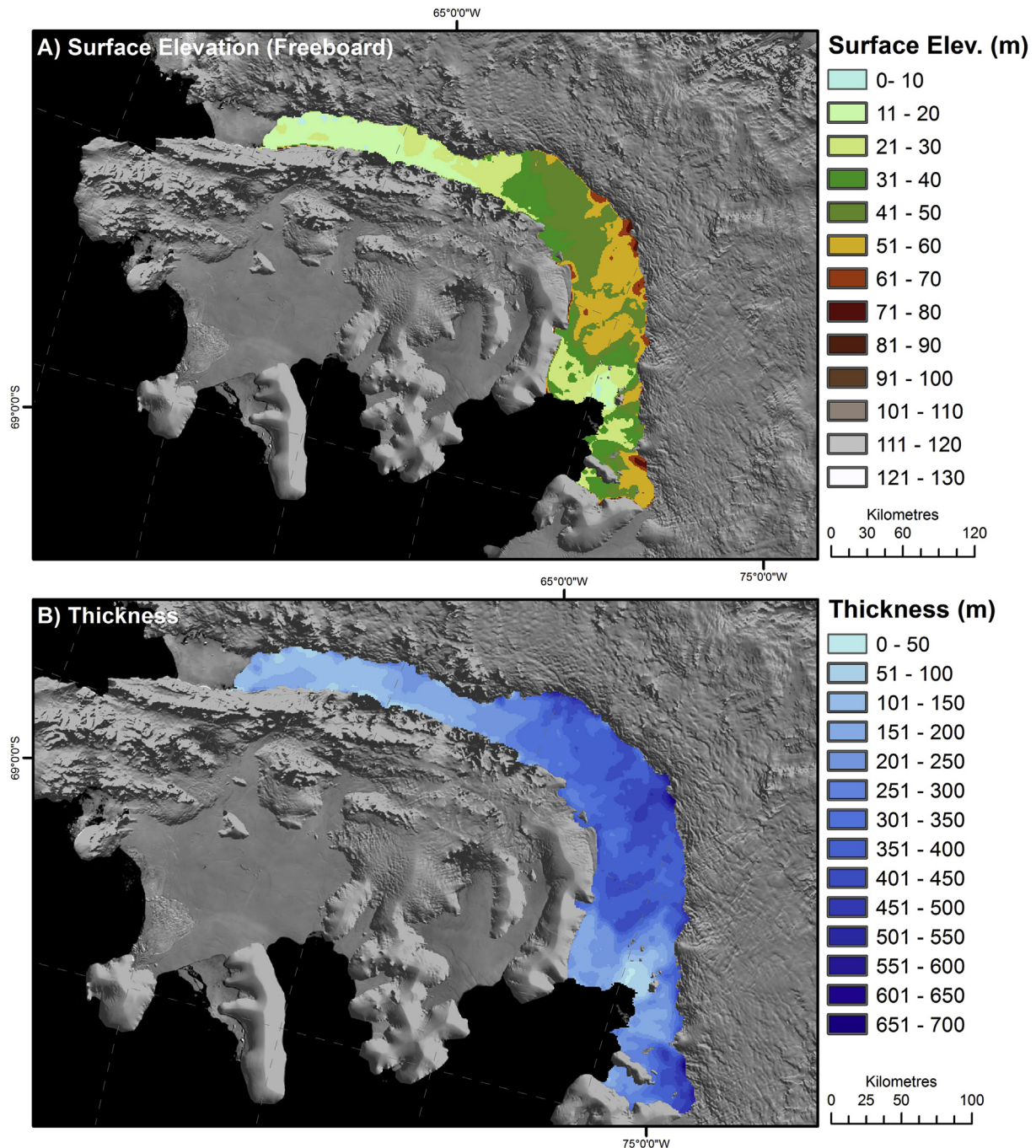


Fig. 3. Modern-day freeboard (A) and ice shelf thickness (B) for George VI Ice Shelf. Surface elevation and ice thickness data from BEDMAP 2 (Fretwell et al., 2013). Images overlain on Mosaic of Antarctica (MOA) (Scambos et al., 2007; Haran et al., 2014).

shelves (Morris and Vaughan, 2003; Vaughan, 2012). The ice shelf is subjected to surface melting each summer, with extensive meltwater ponds developing (Reynolds and Hambrey, 1988; Holt et al., 2013; Hambrey et al., 2015). Surface meltwater ponds such as these have been implicated in the dramatic collapse of ice shelves further north on the Antarctic Peninsula (Scambos et al., 2003, 2009; Glasser et al., 2009). However, GVIIS appears to be stable despite the longstanding presence of surface water. Supraglacial lakes on the ice shelf migrate along the boundary of the ice shelf with Alexander Island, at a different velocity and in a different direction to ice velocity (LaBarbera and MacAyeal, 2011), and are associated with a viscous buckling wave caused by the compressive ice-shelf stresses.

GVIIS has been receding slowly since observations began (Cook and Vaughan, 2010), but remains near equilibrium (Smith et al., 2007a), although there is some acceleration in rates of recession at the northern ice front (Holt et al., 2013). Rates of basal melting are high, related to the intrusion of warm Upper Circumpolar Deep Water beneath the ice shelf (Smith et al., 2007a), although at least one area of basal freezing has been identified at Hobbs Pool (Pedley et al., 1988). The ice shelf is not currently considered to be in imminent danger of collapse, but is vulnerable to ongoing atmospheric and oceanic warming (Holt et al., 2013). The atypical ice-flow regime of the ice shelf, with strong compressive strain rates in regions with surface meltwater ponding, may provide the ice shelf with additional stability (Humbert, 2007; LaBarbera and MacAyeal, 2011). The past response of the ice shelf to environmental change and any conditions that caused past ice-shelf breakup are therefore of substantial scientific interest.

GVIIS is under compression, with ice-flow directed from the west to the northwest (Fig. 2). At Ablation Point Massif, the ice shelf ice originates from Palmer Land and flows westwards, impinging against Alexander Island (Hambrey et al., 2015). The marginal zone around Ablation Point Massif has previously been described as 'pressure ice', with a series of parallel ridges extending ~2 km from land (Sugden and Clapperton, 1981). Hambrey et al. (2015) reinterpreted these ridges (photographed in Fig. 4) as forming from differential ablation of coarse-clear and white bubble-rich ice. The coarse-clear ice is derived from water-filled crevasses formed in the lower reaches of the source glaciers, which are healed and transposed as they flow across the Sound. The water ice and glacier ice have differing albedos, with the coarse-clear ice preferentially melting, resulting in high-relief topography with ridges parallel to the prevailing crevasse trace-related foliation (Hambrey et al., 2015). There is no evidence of thrusting at Ablation Point Massif, as suggested by Sugden and Clapperton (1981), although this may be an important glaciotectonic process further south at Moutonnée Lake where the ice impinges on Alexander Island. These ice-shelf ridges are associated with ice-shelf moraines on the headlands around Ablation Point Massif, Fossil Bluff and Two Steps Cliffs on Alexander Island (see Figs. 2 and 4 for locations).

At Ablation Point Massif, GVIIS impounds two epishelf lakes in Ablation and Moutonnée valleys (Fig. 4). These epishelf lakes have surfaces close to sea level with a direct hydraulic connection to the sea (Smith et al., 2006a). Both lakes are subject to tidal displacement, resulting in a tidal crack around the edge of the perennial frozen lakes. At the mouths of the lakes, GVIIS is partially grounded on a submerged bedrock ridge. The grounding zone is expressed by a raised crevassed area on the surface of the ice shelf (Smith et al., 2006a). Part of the ice shelf flows westwards over the ridge and into Ablation Lake as a prominent, heavily fractured ice tongue extending 2.8 km into Ablation Lake, resulting in 5 m high ridges of ice (Fig. 4A, B, C, E) (Smith et al., 2006a; Hambrey et al., 2015).

Within the epishelf lakes, meltwater from onshore Alexander Island and GVIIS forms a layer of fresh water across the epishelf

lakes. Meltwater and snow from the catchment will typically accumulate in epishelf lakes until the thickness of the freshwater layer is equal to the minimum draft of the ice shelf. Excess of freshwater inflow is exported below the base of the ice shelf to the sea (Hamilton et al., 2017). Marine waters are advected from beneath the ice shelf. Perennial thick ice cover on the lake surface and strong density stratification prevents mixing and strong convection currents (Veillette et al., 2008).

These two epishelf lakes are characterised by a stratified water column, with a less dense, cold freshwater layer overlying marine water, and are nutrient limited and deficient in phytoplankton (Smith et al., 2006a). A lake-ice conveyor, driven by the pressure exerted on the lake by the ice shelf calving into it and by thermal convection within the lake (Hendy et al., 2000), is hypothesised to transport englacial and supraglacial clasts across the lake-ice surface from the ice-shelf margin, across Ablation Lake to the opposite, western shore (Smith et al., 2007b).

Both epishelf lakes are dependent on the presence of George VI Ice Shelf and would disappear and become marine embayments if the ice shelf was absent (Smith et al., 2007a). The absence of the ice shelf would see the stratified fresh-water column being replaced by marine waters only (Smith et al., 2006a). They are therefore potential indicators of ice-shelf loss. Epishelf lake sediment records bearing marine fauna from Moutonnée Lake suggest that the ice shelf was absent from 9600 to 7730 cal. yr BP (Smith et al., 2007b). Barnacles living in open water at Two Step Cliffs found in ice-shelf moraines below 50 m asl suggest that George VI Sound was also seasonally free of ice from 6850 to 6550 cal. yr BP (Hjort et al., 2001). Smith et al. (2007b) suggest that this indicates a gradual retreat of the northern ice front. Epishelf lakes, which maintain a connection to the ocean, are also important indicators of modern and palaeo sea level (Galton-Fenzi et al., 2012; Hamilton et al., 2017).

2.3. Glacial history

During the Last Glacial Maximum (LGM), Marguerite Trough Ice Stream flowed north out of George VI Sound (Fig. 1) (Ó Cofaigh et al., 2005a; Jamieson et al., 2012), but its thickness and the subsequent glacial unloading is poorly constrained, with only limited relative sea-level data available (Roberts et al., 2009; Whitehouse et al., 2012b). Numerical models suggest that the ice stream was ~1000–1500 m thick at Ablation Point Massif (Jamieson et al., 2012; Whitehouse et al., 2012a; Golledge et al., 2014). Marine geophysical and onshore geomorphological observations suggest that Alexander Island supported an independent ice cap at the LGM (Sugden and Clapperton, 1980; Clapperton and Sugden, 1982, 1983; Graham and Smith, 2012; Johnson et al., 2012), with an ice divide located along the north-south line of high mountains. Data-calibrated numerical models also support thick ice over Alexander Island at the LGM (Golledge et al., 2014; Jamieson et al., 2014), but sparse regional evidence of ice thickness limits these models. Cosmogenic nuclide ages of 30 ka in Moutonnée Valley place the Alexander Island Ice Cap ice surface at 600 m asl at the global LGM (Hughes et al., 2013), falling to 500 m asl by 11.9 ka (Bentley et al., 2006). Ages obtained from northern Alexander Island nunataks suggest that 490 m of thinning was initiated at 21.7 ka until 10.2 ka, at a rate of 2.2 cm a⁻¹ (Johnson et al., 2012).

The post-LGM recession of the grounding line of Marguerite Trough Ice Stream is unclear. Marine sediment cores from the continental shelf suggest that the ice stream had retreated from the mid-shelf by ~14 cal ka BP (Ó Cofaigh et al., 2014). There is a relatively wide spread of ages (Fig. 1). These marine radiocarbon ages are minimum ages, as they are the first datable organic material in the glaciomarine sediments; therefore deglaciation occurred

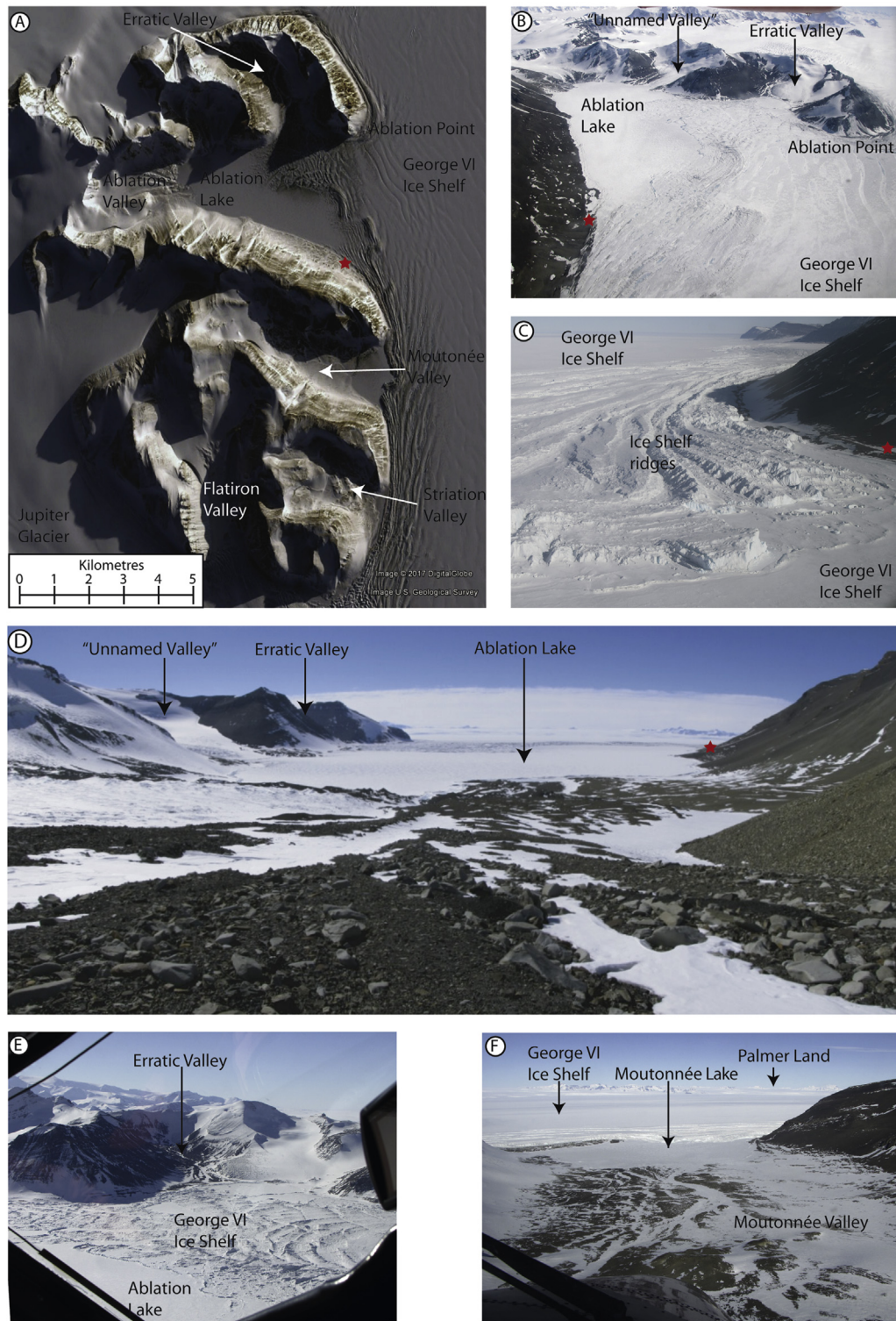


Fig. 4. Location photos of the study area. Red star indicates location of Basecamp. A: Digital Globe 2017 image from Google Earth Pro of Ablation Point Massif. B, C: Oblique aerial photographs of Ablation Valley. In C the ice-shelf ridges (~20 m amplitude) are clearly visible. They curve out into the centre of the lake, where the direction of lake-ice movement is fastest. D: Looking down Ablation Valley, towards the ice shelf. E: Oblique aerial photograph of Ablation Lake and Erratic Valley. Note the arcuate ridges of sublimating calved icebergs from GVIIS within the lake ice. F: Oblique aerial photograph looking down Moutonnée Valley, across Moutonnée Lake and over GVIIS to Palmer Land on the far horizon. (For interpretation of the references to colour in this figure legend, the reader is referred to the web version of this article.)

earlier and the ice stream retreated before this time. Where basal ages among different cores are scattered, the oldest ages are therefore most likely to be accurate. Lake sediment records from Moutonnée Lake suggest that George VI Sound was clear of ice at

this location by 9.6 cal ka BP, when marine sedimentation commenced (Smith et al., 2007a, 2007b). Together, these data suggest rapid ice-stream recession up Marguerite Trough and into George VI Sound during the early Holocene. The terrestrial geologic

record presents an excellent opportunity to further refine estimates of rates of ice-stream recession and the commencement of glacio-marine conditions in George VI Sound.

Geomorphological evidence indicates that after the LGM, valley glaciers in Ablation Valley extended well into George VI Sound, depositing a “Valley Till” (Clapperton and Sugden, 1982, 1983). Palmer Land erratics superimposed on the “Valley Till” at Ablation Point Massif indicate later overprinting by the ice shelf, with exotic boulders distributed across some 60 km: at Ablation Point Massif up to an elevation of 81 m, Fossil Bluff to 85 m and Two Steps Cliffs to 110 m (Clapperton and Sugden, 1982; Smith et al., 2007a). These palaeo ice-shelf moraines are overlain by ice-cored valley glacier moraines at Ablation Point Massif, interpreted as a Late-Holocene readvance. In Erratic Valley, multiple valley glacier fluctuations are documented by overlapping ice shelf and valley glacier moraines (Clapperton and Sugden, 1982, 1983).

The high-elevation palaeo ice-shelf moraines at Ablation Point Massif (up to 81 m asl) are generally assumed to be Holocene in age (Clapperton and Sugden, 1982; Smith et al., 2007b), but are undated. Elsewhere along the eastern coast of Alexander Island, amino acid racemisation of *Hiatella solida* shells in ice-shelf moraines at 110 m at Two Steps Cliffs (Fig. 1) gave a single shell specimen an age of 120 ka, but this technique has since been refined and previous ages are often considered unreliable (Penkman et al., 2007). Clapperton and Sugden (1982) interpreted this as a reworked shell, and gave the ice-shelf moraines at Two Steps Cliffs a provisional age of around 80 ka. Thus the ages of the Alexander Island ice-shelf moraines are poorly constrained.

The few regional sea level records include a raised delta in Ablation Valley, which places the local relative sea level at 14.4 m asl at 4.6 ± 0.4 ka (Roberts et al., 2009). Records from Narrows Lake on Pourquoi Pas Island, Marguerite Bay, suggest that regional sea level was 19.4 m at 6.5 cal ka BP (Bentley et al., 2005a). Optically stimulated luminescence dating on cobbles from raised beaches in Calmette Bay indicate that the Holocene marine limit was 21.7 m asl, with an age of 5.5–7.3 ka (Simkins et al., 2013). On Horseshoe Island, a lake basin at 3.5 m asl became isolated from marine influences at 1.3 ± 0.2 cal ka BP (Wasell and Håkansson, 1992).

Key uncertainties include the ice thickness and timing of recession of Marguerite Trough Ice Stream; the poorly resolved chronostratigraphy and complex interaction between valley glaciers and the ice shelf (Clapperton and Sugden, 1982, 1983); the relationship between limnological records from Ablation Lake and Moutonnée Lake (Roberts et al., 2008) and the onshore geomorphological record. Palaeo sea levels are poorly understood, with just one data point recorded in this region (Roberts et al., 2009; Whitehouse et al., 2012b), and the age of the highest ice-shelf moraines is unconstrained.

3. Methods

3.1. Field surveys

Field mapping and sampling were undertaken at Ablation Point Massif on Alexander Island, western Antarctic Peninsula. Mapping focused on Ablation Valley, Erratic Valley and Moutonnée Valley (Fig. 4). Initial mapping was completed using satellite imagery and aerial photographs, ground-checked and georeferenced during fieldwork (November 2012). A handheld GPS, accurate to ± 10 m horizontally, was used for geopositioning. Altitudes were checked with the GPS and a barometer.

A range of standard sediment analysis techniques were performed, including analysis of moraine shape and morphology, and clast form and roundness (Powers, 1953; Hubbard and Glasser, 2005; Hambrey and Glasser, 2012) on sets of 50 gravel clasts,

analysed using triplots and the RA/C₄₀ index (cf. Benn and Ballantyne, 1994; Benn, 2007). RA (aggregate roundness) is the percentage of very angular to angular clasts within a sample. C₄₀ (aggregate shape) is the percentage of clasts with *c/a* axial ratios of ≤ 0.4 . Each datapoint represents the calculated RA-C₄₀ values for one sample (≥ 50 stones). Sediments and lithofacies were described and mapped in detail, following standard protocols (Hambrey and Glasser, 2003).

3.2. Clast provenance

The full range of exotic and local clasts were sampled from moraines adjacent to Ablation Lake and Moutonnée Lake, and analysed for provenance using thin sections. In almost all of the clasts examined, a Palmer Land or Alexander Island provenance was clearly defined by the textural or mineralogical characteristics (Supplementary Table 1; see also Hambrey et al., 2015). The principal distinguishing features are summarised here.

Palmer Land erratics were most commonly coarse plutonic rocks, mainly tonalites and quartz diorites but also rarer granite and diorite. They were derived from the Antarctic Peninsula batholith in northern Palmer Land. Analogous plutonic rocks in Alexander Island crop out mainly in the far north of the island and west of the major topographical divide. They are thus unlikely to have contributed clasts to eastern Alexander Island.

Pluton-derived clasts are distinguished from Palmer Land metamorphic basement by an absence or weak development of a foliation and absence or minimal development of recrystallization. Palmer Land basement is represented by strongly foliated amphibolite, diorite and tonalitic gneiss, and quartzose phyllite; quartzo-feldspathic mosaics and marginal recrystallization of feldspar crystals are also conspicuous, together with fine quartzo-feldspathic veins resembling mylonite.

With the exception of well-rounded lava pebbles, which were reworked from the Fossil Bluff Group of Alexander Island, angular basaltic and andesitic lavas and hypabyssal rocks, and dacitic pyroclastic rocks, are confidently assigned to the two major Jurassic and Cretaceous volcanic groups in Palmer Land since outcrops of volcanic strata in Alexander Island are situated to the west of the LeMay Range topographical divide. By contrast, clasts of well sorted arkoses and rarer immature volcanolithic sandstones were sourced in the Fossil Bluff Group of Alexander Island. They are metamorphosed to prehnite-pumpellyite facies and some contain chlorite-altered volcanic glass, which are also distinctive characteristics of the Fossil Bluff Group.

3.3. Cosmogenic nuclide dating

Cosmogenic ^{10}Be and ^{26}Al dating is widely used to date moraines (Gosse and Phillips, 2001), ice volume changes and ice sheet thinning around nunataks (Bentley et al., 2006, 2010). Samples were collected from the top surface of glacially transported boulders (Gosse and Phillips, 2001; Balco, 2011), from moraine crests or from flat benches on hill slopes, where there was minimal possibility of rolling or rotation. We sampled boulders with ample signs of glacial abrasion (rounding, faceting or striations), which should favour the removal of inherited nuclides. As the mapped facies occur as a drift with a series of subtle mounds rather than discrete, clear ridges, it was not possible to obtain multiple replicate samples from individual moraine crests. Suitable boulders for dating are also rare. Rather, we focused our efforts on obtaining clear altitudinal transects. Thus the samples form a coherent dataset at different elevations across a sediment-landform assemblage.

Prior exposure and recycling from older deposits frequently results in anomalously old exposure ages (Bentley et al., 2006;

Balco, 2011; Johnson et al., 2012). A significant difficulty in Antarctica is the possibility of transport or burial by cold-based ice, resulting in complex exposure histories. In order to rule out long complex exposure-burial histories, ^{26}Al and ^{10}Be concentrations have been compared to the cosmogenic $^{26}\text{Al}/^{10}\text{Be}$ production rate ratio. Following convention in Antarctica, in the case of geologic scatter, we assume that the youngest age is most likely to be correct, as inheritance is the most likely cause of anomalously old ages (cf. Bentley et al., 2006). Outliers may also occur as a result of rolling or boulder rotation, which may result in anomalously young ages. Anomalously young ages can also be produced if samples are snow- or debris-covered, or are exhumed from moraines (Putkonen and Swanson, 2003). An initial screen using the isotopes ^{26}Al and ^{10}Be was used to identify any discordant ages that might imply previous complex exposure (cf. Bentley et al., 2006; Corbett et al., 2011). If the sample is buried, the two isotopes will decay at different rates, and the isotopic ratio between the two will evolve from its initial production value (6.75).

The ^{10}Be concentrations are based on 2.79×10^{-11} $^{10}\text{Be}/\text{Be}$ ratio for the NIST SRM4325 AMS standard, and the ^{26}Al concentrations are based on 4.11×10^{-11} $^{26}\text{Al}/\text{Al}$ ratio for Z92-0222 AMS standard. Blank corrections ranged between 3 and 35% of the sample $^{10}\text{Be}/\text{Be}$ ratios, and between 0.1 and 3.8% of the sample $^{26}\text{Al}/\text{Al}$ ratios. The sea-level high-latitude (SLHL) production rate reference is given by the CRONUS-Earth online calculator version 2.3 and the scaling scheme used. In this case, the SLHL ^{10}Be production rate due to spallation for the time-dependent Lal/Stone (Lm) scaling scheme in the CRONUS-Earth online calculator version 2.3 was 4.39 ± 0.37 atoms/g/yr. The uncertainty of these corrections are included in the stated standard uncertainties. The ^{26}Al standard uncertainties also include between 1.4% and 1.9% for the uncertainty of stable Al determination. Exposure ages, internal uncertainties and topographic shielding were calculated using the CRONUS-Earth online calculator version 2.3 (Balco et al., 2008). Topographic shielding was calculated by measuring the angle to the horizon at 20° azimuths. A rock density of 2.65 was used. An erosion rate of 0 was applied, as erosion rates are poorly quantified. In addition, the preservation of striations, edge rounding and facets on the sampled boulders supports negligible erosion. However, applying an erosion rate of 1 mm/kyr, the high end for Antarctic sandstones (cf. Hein et al., 2016), would increase our ages by less than 400 years for the oldest ages, a difference of 1.7% and well within the uncertainties of the ages. For a maximum high estimate of 2 mm/kyr, we observe a difference of 728 years (3.4%) and still within the sample analytical uncertainties. We therefore argue that our samples are insensitive to the application of an erosion rate. Antarctic low atmospheric pressure was considered in the calculations (Stone, 2000). We present full sample details used to calculate ages in the Supplementary Information. Results using the time-dependent Lal/Stone scaling scheme are shown.

Five of the prepared Al AMS samples yielded low ^{27}Al current and the precision of these measurements could not be stated by comparing with the AMS standards used. These concentrations are therefore not shown here. However, considering the scatter of the raw AMS data as uncertainties, the average $^{26}\text{Al}/^{10}\text{Be}$ ratios obtained from these samples were also indistinguishable from the production rate ratio.

4. Sediment-landform associations

4.1. Drift with Alexander Island erratics

The oldest, highest stratigraphic unit at Ablation Point Massif is a drift (i.e., a continuous and extensive deposit of glacial till) with Alexander Island erratics. This drift is located above the elevation of

the 'Drift with Palmer Land erratics' and lacks Palmer Land erratics (Fig. 5). On "The Mound" (an informal, unofficial name) at the head of Ablation Valley (Fig. 6), at 240 m asl, it is characterised by angular, local clasts and surficial sediments comprising silty sand with a lag of pebble-cobble gravel. It is similar to drift observed in other parts of the Antarctic Peninsula (Davies et al., 2013; Glasser et al., 2014). In Moutonnée Valley, this drift is associated with roches moutonnées aligned down the axis of the valley, representing ice flow by Alexander Island ice (Fig. 5). The roches moutonnées in Moutonnée Valley are quarried on multiple sides, primarily on their eastern and northern faces, and their form is strongly controlled by jointing.

Near the coast in Moutonnée Valley, striations in the basaltic bedrock near the coast indicate east-west ice flow that cuts across modern north-south ice flow, primarily east-west, indicating a different ice-sheet configuration during this stage.

We interpret this drift as representing local glaciation of Alexander Island, with glaciers flowing down-valley and into George VI Sound, where they were confluent with Marguerite Trough Ice Stream, which flowed north to the continental shelf edge (Jamieson et al., 2012, 2014). At the coast in Moutonnée Valley, striations in basalt bedrock were likely emplaced by Marguerite Trough Ice Stream. In Ablation Valley, the character of the drift on "The Mound" suggests that it was emplaced by cold-based glaciers (Atkins, 2013), when a larger glacier occupied the glacially sculpted valley.

4.2. Ice-cored ice-shelf moraines

The modern ice-shelf moraines are thoroughly described by Hambrey et al. (2015), and so are only summarised here. Ice-shelf moraine wraps around the headlands of Ablation Point and Moutonnée Point (Fig. 5; Fig. 7). These large ice-cored ice-shelf moraines are associated with structurally controlled ice ridges on the ice shelf and are characterised by granite erratics from Palmer Land, and by striated and faceted pebbles (Fig. 8), and a silty diamicton less than 1 m thick (see Fig. 7). Pebbles are commonly edge-rounded with a blocky shape. The ice-cored moraine comprises a veneer of clast-rich sandy diamicton and sandy gravel, from a few centimetres to a few metres in thickness, overlying ice-shelf ice (Fig. 7A). The ice-shelf moraines comprise both 'active', sharp-crested, ice-cored moraines (Fig. 7B) and degraded moraines with no ice core (Hambrey et al., 2015).

Palmer Land boulders commonly greater than 1 m in diameter are scattered over the ice-cored moraine, and up to 20% of gravel clasts are derived from Palmer Land (Fig. 8) although the proportion of erratic clasts is highly variable spatially. A representative sample of clasts from the ice-cored moraine in Ablation Valley examined by thin section revealed quartz diorite, tonalite and granodiorite from the Antarctic Peninsula batholith, basalt lava and sandstones from the Fossil Bluff Group on Alexander Island (Sample L12.257.1; Supplementary Table 1). Boulders from the local Fossil Bluff Group, such as pebbles of basaltic and andesitic lavas, sandstones and siltstones, are found intermixed with these erratics. At Moutonnée Point, the far-travelled rock assemblage of the ice-shelf moraine (sample L12.227; Supplementary Table 1) includes sheared recrystallized diorite, diorite, meladiorite, tonalite, gneiss and granite, all deriving from Palmer Land.

The ridges on the ice shelf have ice with a near-vertical foliation and a relief of ~20 m. As the ice ablates by sublimation or melting, sediment collapses to form debris flows; once the ice core is melted, resulting landforms are near-horizontal, subdued, levelled benches. Erratic clasts were transported from Palmer Land either englacially, or at the base of the ice shelf during a period of decreased basal melting and increased basal freezing (Hambrey

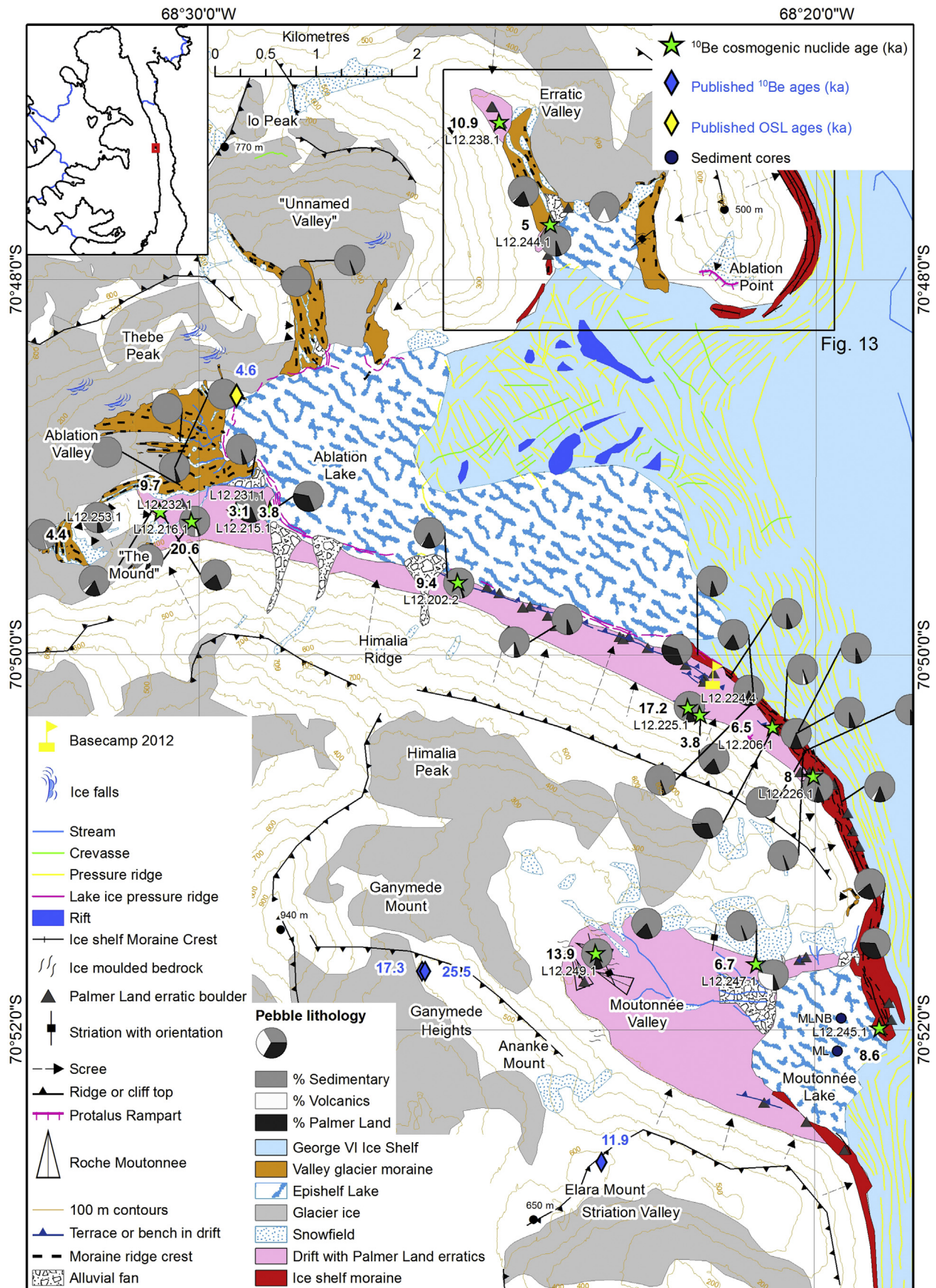


Fig. 5. Location map and geomorphological map of Ablation Point Massif, showing the principal stratigraphic units. Pie charts show percentages of clast lithologies from different domains. Published ^{10}Be and OSL ages (in ka) from Bentley et al. (2006) and Roberts et al. (2009) respectively. Moutonnée Lake sediment cores from Smith et al. (2007b). 100 m contours are derived from ASTER GDEM version 2.

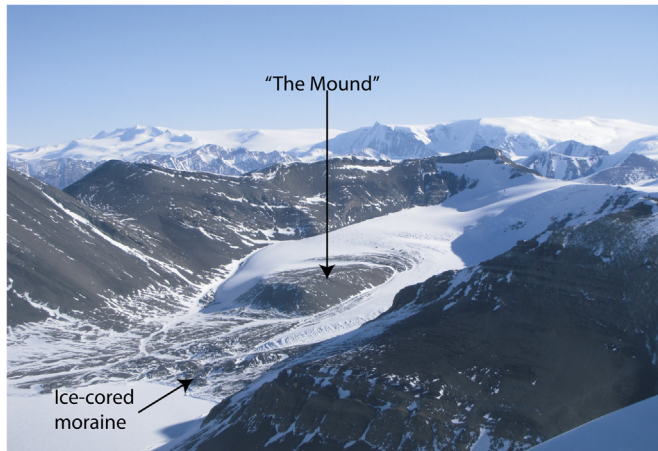


Fig. 6. Oblique aerial photograph of “The Mound” at the head of Ablation Valley.

et al., 2015).

Where the ice shelf is grounded against Alexander Island, local debris is incorporated (Hambrey et al., 2015). Actively forming scree and colluvium occur inland of the degraded moraines and some angular locally-sourced boulders and other debris are added onto the moraines via this mechanism. The sediments are therefore a combination of local and exotic material, with a proportion of fines incorporated by the wet-based glaciers on Palmer Land (Hambrey et al., 2015). In contrast, at Fossil Bluff (Fig. 1), valley glaciers contribute to the ice shelf, resulting in ice flow away from Alexander Island and an absence of modern ice-shelf moraines (Sugden and Clapperton, 1981; Reynolds and Hambrey, 1988).

4.3. Epishelf lakes

The grounding zone of GVIIS is clearly visible in Ablation and Moutonnée epishelf lakes as a series of ice ridges, which extend well into the lakes (Fig. 4). The ice shelf gradually fragments into Ablation Lake as icebergs, which sublimate to form low ridges (Fig. 4; Fig. 9A), as has been observed in other ice-dammed lakes in Antarctica (Hall et al., 2006). These low ridges of calved icebergs, originally formed perpendicular to the calving front, become increasingly arcuate towards the centre of the lake.

Surrounding the margin of Ablation Valley epishelf lake are two small ice-ridges where the lake ice has been thrust up to 2 m high around the lake margin (Fig. 9A). These ridges are associated with a tidal crack, where displacement occurs daily in accordance with the tides. The inner thrustured lake ice has a vertical crystal structure and

mostly is very clean ice, with limited debris load (Fig. 9B and C).

The outer ridge is composed of thrustured and reworked local sediments (Fig. 9D and E), most prominently along the southern margin of the lake, closer to the ice shelf. Here, north-facing slopes of the thrustured ice are covered with a thin layer of coarse diamicton or coarse, poorly sorted material overlying finer sediments (Fig. 9D). When de-iced, these form a low, rounded, hummocky ridge of poorly sorted sediment overlain by coarse cobbles and gravels, including both locally derived and Palmer Land erratic cobbles and small boulders (Fig. 9E). In most places, these ridges comprise simply reworked local material. There is no evidence of pebble edge-rounding or sorting by wave action on the lake.

We argue that a lake-ice conveyor operates here (cf. Hendy et al., 2000; Hall et al., 2006), whereby icebergs calved into the lake ice gradually sublimate and are subsumed by the lake ice. Icebergs and glacially transported material are moved to the lake edge due to pressure exerted on the lake ice by the ice shelf. In this mechanism, seasonal warming at the lake margins, where the ice is thinner, can cause melting at the margins. A limited convection current likely occurs within the ice; the lake is coldest close to the ice shelf, where fresh meltwater easily freezes. A moat occurs at the lake shoreline during the height of summer; the ice melts and debris within the lake ice is released to the shoreline. The ridges of calved icebergs become increasingly arcuate because the lake-ice conveyor moves faster in the centre of the lake than at the edges (cf. Hall et al., 2006). Debris content of the ice shelf and lake ice is low but erratics and local clasts entrained by the ice shelf (cf. Hambrey et al., 2015) are encased by the lake ice. Pressure from the ice shelf and limited thermally driven convection currents within the lake therefore drive the lake ice conveyor, delivering Palmer Land erratics and local clasts to the shoreline, as observed in Fig. 9D. However, the strongly stratified nature of the lake suggests that there are likely to be limited convection currents and mixing (cf. Laybourn-Parry et al., 2001).

4.4. Drift with Palmer Land erratics

4.4.1. Overview

A drift rich in Palmer Land erratics was mapped above the epishelf lakes and around the coastline of Ablation Lake and in Erratic Valley (Fig. 5). It is widespread in Ablation, Erratic and Moutonnée valleys at elevations below 140 asl. The drift is characterised by a series of indistinct benches or terraces with 10%–38% Palmer Land erratics and a fine-grained silty-sand or diamicton matrix beneath a surficial pebble-cobble lag (Fig. 10). There are particularly prominent terraces at 15–20 m and 5–8 m in all the valleys. Pebbles are commonly blocky, subangular to subrounded, and are frequently striated, bullet-shaped and faceted (Fig. 10;

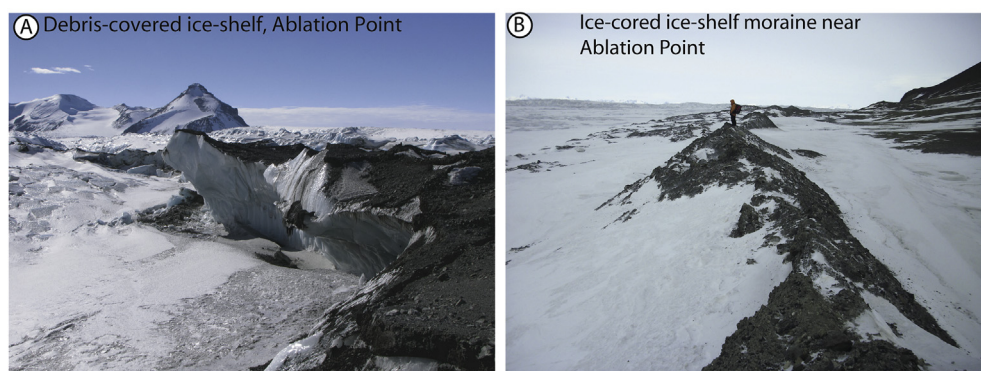


Fig. 7. Ablation Point Massif ice-shelf moraines. A: Thin mantle of debris on George VI Ice Shelf ice at Ablation Point. B: Young, sharp-crested, ice-cored ice-shelf moraines.

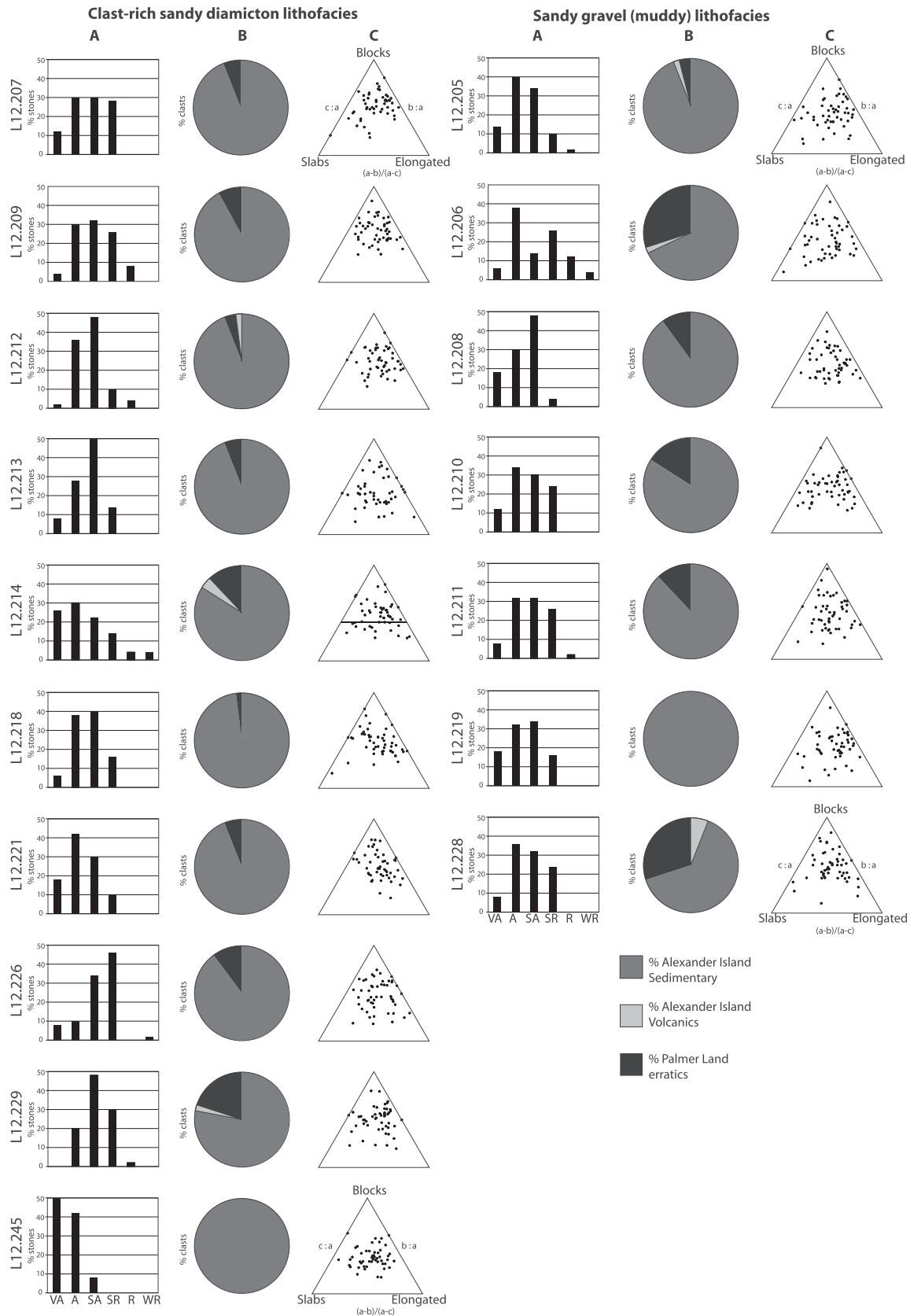


Fig. 8. Representative data for current ice-shelf moraines at Ablation Point and from near basecamp (cf. Fig. 5), showing the clast-rich diamicton and sandy gravel lithofacies. After Hambrey et al., 2015. Column A: Percentage clasts in each roundness category (Very Angular, Angular, Subangular, Subrounded, Rounded, Well rounded). Column B: Clast shape ternary plots. Column C: Percentage clasts in different lithological categories (Sedimentary, Volcanics, Palmer Land erratics).

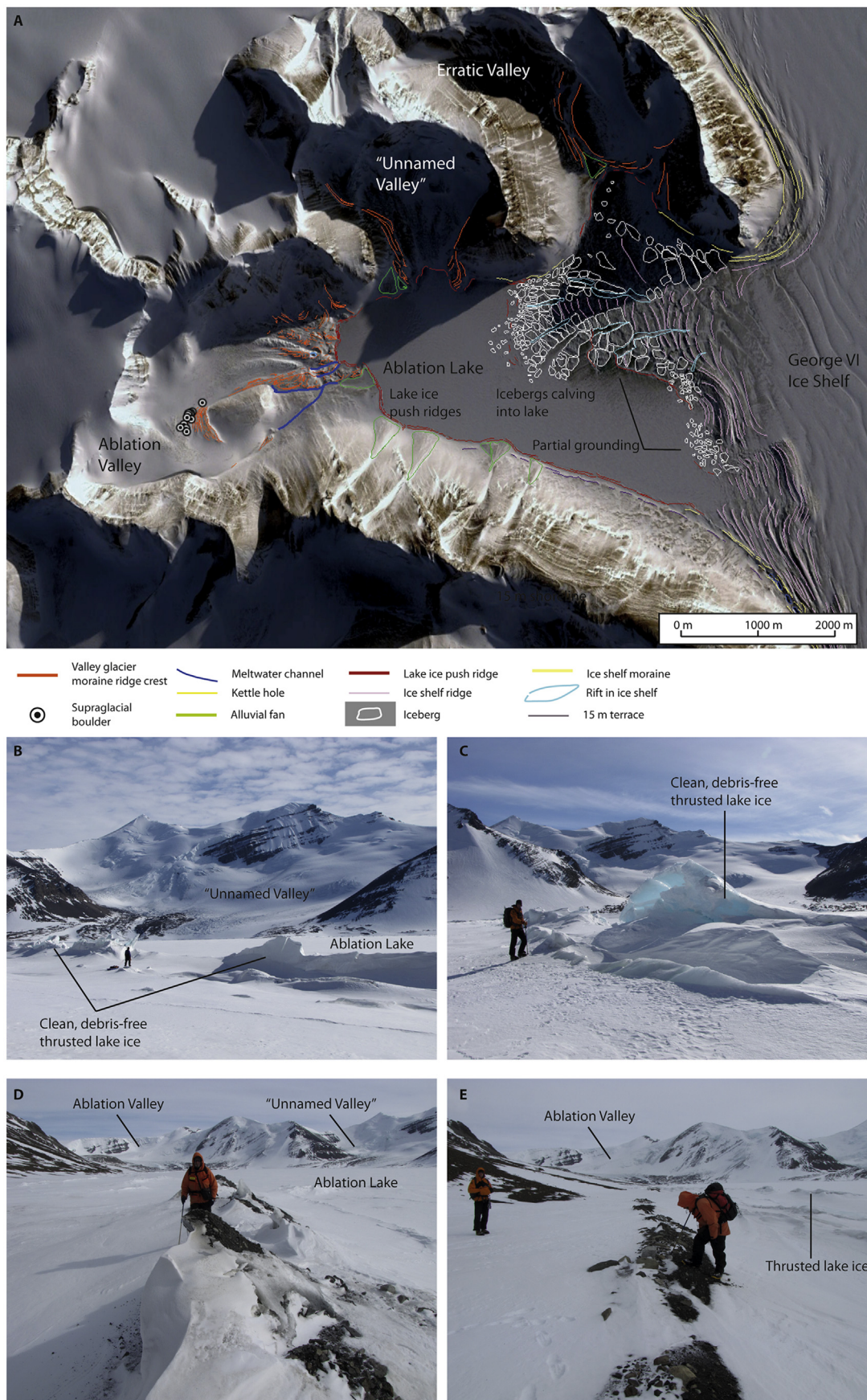


Fig. 9. Lake-ice push ridges in Ablation Valley. **A.** Digital Globe image from Google Earth Pro showing two concentric lake-ice pressure ridges (red lines) at the head of Ablation Valley and icebergs (white) from George VI Ice Shelf calving into the lake. Ice shelf is partially grounded, as shown by the pink ridges of ice. **B, C:** Lake ice thrust up into high ridges at the head of Ablation Valley at the edge of the lake (the ridges visible in **A**). Note the lack of debris visible on or within the ice. **D:** Lake ice, pushed up into sub-vertical ridges along the margin of the epishelf lake. **E.** Small ridge along the margin of the epishelf lake. Note the cluster of cobbles, including far-travelled Palmer Land erratics, along the ridge-crest. Lake ice ridges are visible to the right of the low ridge. (For interpretation of the references to colour in this figure legend, the reader is referred to the web version of this article.)

Drift with Palmer Land erratics (representative samples)

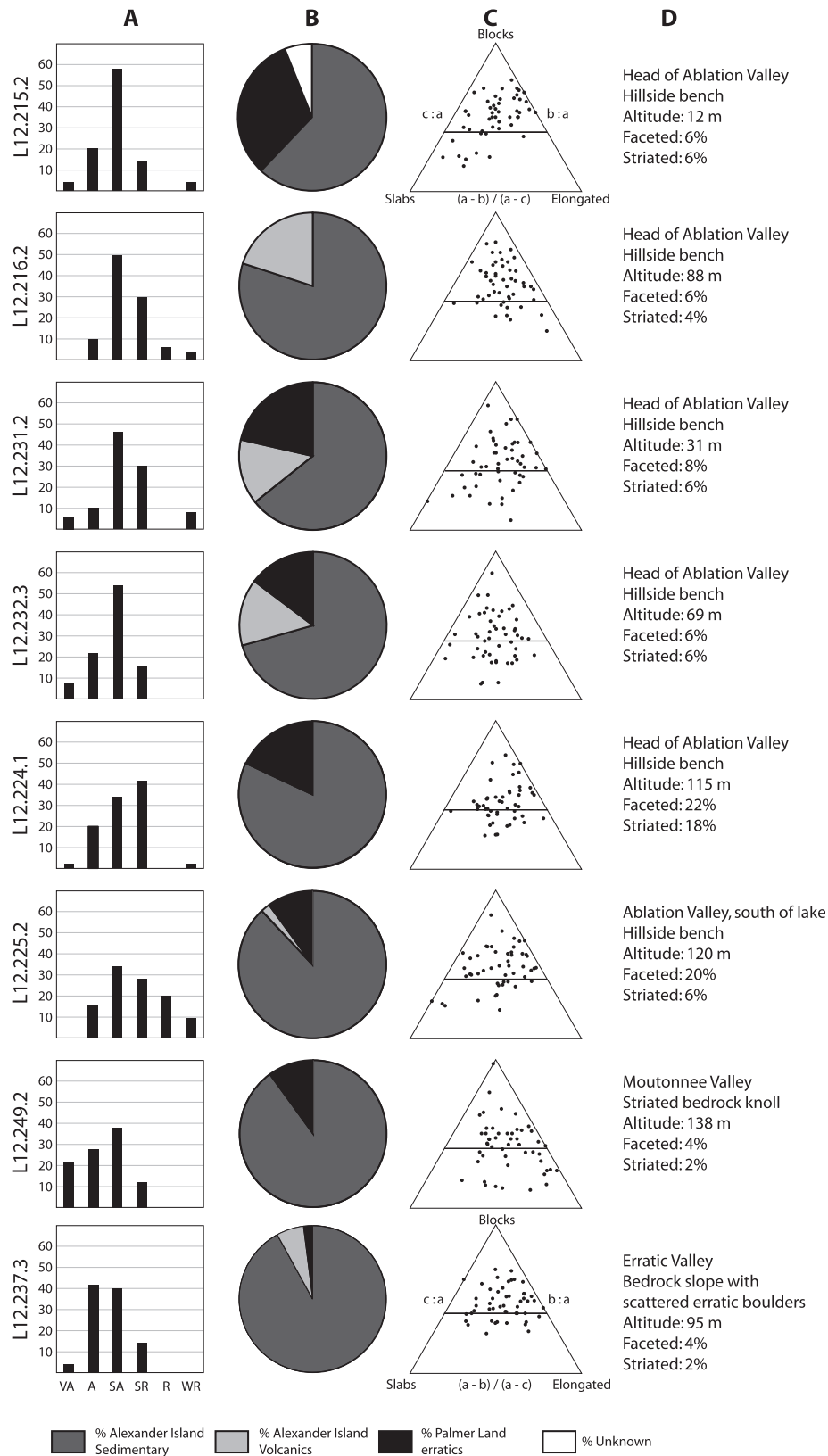


Fig. 10. Representative clast data from the Drift with Palmer Land erratics. Column A: Percentage clasts in each roundness category (Very Angular, Angular, Subangular, Subrounded, Rounded, Well Rounded). Column B: Percentage clasts in different lithological categories (Sedimentary, Volcanics, Palmer Land erratics, and unknown). Column C: Clast shape ternary plots. Column D: Details of sample location and percentage of clasts that are striated or faceted. See Fig. 8 to compare with present-day ice-shelf moraines. See Fig. 5 for locations listed in column D.

Fig. 11). Surficial sediments and stone angularity-roundness data from this erratic-rich drift are indistinguishable from the modern ice-cored ice-shelf moraine as described by Hambrey et al. (2015) (compare Figs. 8, 10 and 11). Within the drift, there are occasional large, typically faceted and edge-rounded Palmer Land granite boulders (boulders with an a axis greater than 1 m are shown on Fig. 5) as well as numerous locally derived rocks and pebbles. In places the Drift with Palmer Land erratics is overprinted with scree, periglacial slope deposits (colluvium), epishelf lakes and alluvial fans.

4.4.2. Ablation Valley

Towards the seaward edge of Ablation Lake, in the vicinity of our basecamp, the drift with Palmer Land erratics is contiguous with, and grades into, the modern ice-cored ice-shelf moraines that bound the eastern edges of Ablation Point Massif, where GVHS abuts Alexander Island. Directly above the modern ice-shelf moraine at this location, a series of ridges are present on the hillside at elevations of up to 120 m asl (Fig. 12A and B). These distinct ridges (30 m wide, with a clear 1 m high ridge at the distal slope) comprise a clast-rich diamicton, have several granite cobbles to boulders on the ridge crests, and 18% of the gravel component are Palmer Land erratics (L12.224.1 and L12.225.2; Fig. 10). Thin sections of rock samples collected from the ridge revealed recrystallized andesite and pyroclastic rock from the Palmer Land Volcanic Group, tonalite and quartz diorite from the Antarctic Peninsula batholith and andesite lava and silica-rich andesite which could derive from the Antarctic Peninsula Volcanic Group or the Palmer Land Volcanic Group (both from Palmer Land) (Supplementary Table 1). There are also numerous locally derived cobbles, many

of which bear striations.

At the western head of Ablation Valley, the drift occurs as a series of cross-valley benches and drift mounds that contour around the valley at elevations of up to 90 m. It is overprinted by valley glacier ice and moraines. The drift with Palmer Land erratics here comprises rare scattered erratic cobbles and small well embedded boulders. Slope and frost sorting processes are active. Palmer Land erratics comprise ~20% of the gravel content in stone counts (Fig. 11B). At 69 m asl, several Palmer Land granite and Palmer Land quartz diorite boulders (Supplementary Table 1) rest on a bench in the hillside (sample L12.232.3; Fig. 10). The bench is discontinuous but contours around the hillside. The surficial sediments here are diamicton with mostly local cobbles and boulders but 2% Palmer Land erratics. A lower bench at 31 m asl also contains numerous Palmer Land erratics on a coarse, poorly sorted sandy gravel, with a lag of pebbles on the surface. The discontinuous bench curves around the hillside, with both rounded red-stained granite cobbles (from the local conglomerate) and subangular to subrounded white granites with characteristic plagioclase feldspar and amphibole xenoliths (from Palmer Land).

In Ablation Valley, there is a prominent bench >20 m wide within the erratic-rich drift at 15–20 m asl, littered with Palmer Land erratic boulders (e.g., Fig. 12A; C). The terrace extends prominently down the side of Ablation Valley (Fig. 5). It has a smooth slope covered with a deflated pebble-cobble gravel with numerous large boulders and erratics (Fig. 12D). Periglacial stone stripes are well developed across the surface. The slope dips down at ~10° towards Ablation Lake. The boulders embedded within the surficial sediments are generally rounded to sub-rounded. They are located too far from the slopes above to have arrived in their current

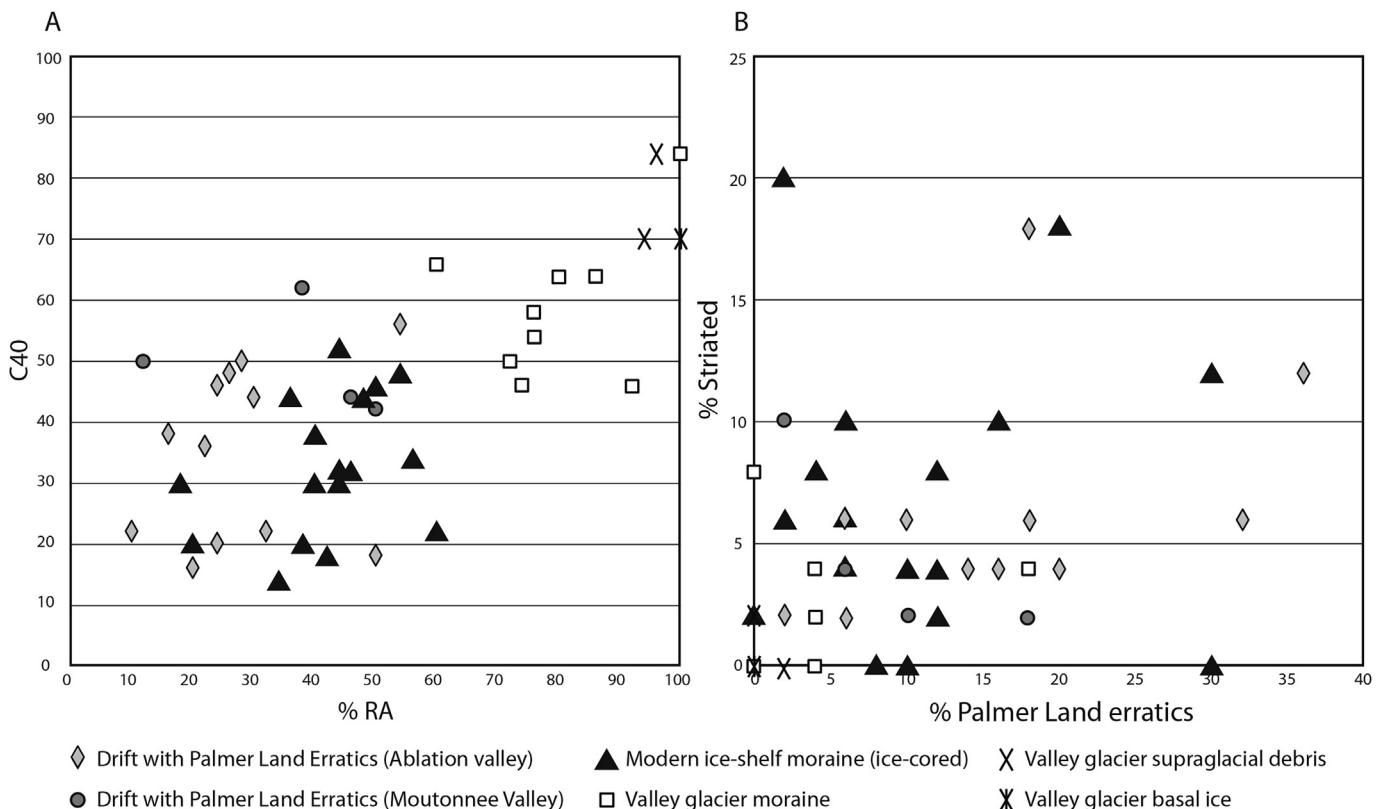


Fig. 11. A. RA-C₄₀ plot for different lithofacies at Ablation Point Massif, showing a strong overlap in clast shape-roundness between palaeo and modern ice-shelf moraines (cf. Benn and Ballantyne, 1994; Benn, 2007). RA is aggregate roundness, C₄₀ is aggregate shape. Each datapoint represents the RA-C₄₀ values for one sample (≥ 50 stones). B. Percentage Palmer Land Erratic versus percentage striated pebbles in each surficial stones sample ($n = 50$). Drift with Palmer Land Erratics is indistinguishable from the modern ice-shelf moraine. Some valley glacier moraines contain reworked Palmer Land erratics where the valley glaciers have overridden the Drift with Palmer Land erratics.

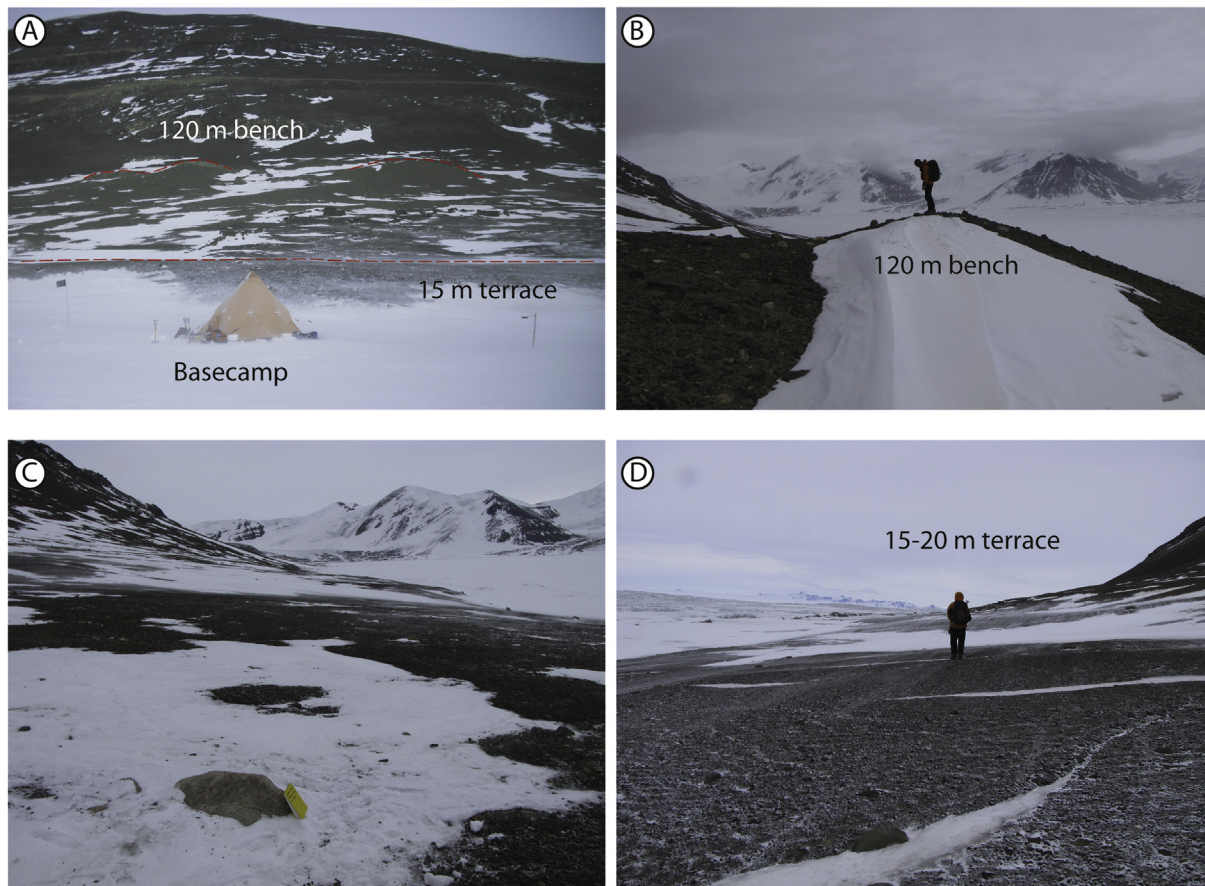


Fig. 12. A. Basecamp, towards the mouth of Ablation Valley, with a clear 15 m terrace and a clear 120 m terrace above. B. Ridge at 120 m asl on hillside directly above ice-shelf moraines and basecamp. Site of samples L12.115 and L12.226. C. The 15–20 m terrace, looking towards Ablation Valley. Palmer Land granite boulder in foreground. D. 15–20 m terrace, looking towards the ice shelf. Palmer Land mountains visible in the distance.

locations by slope processes or rolling; a cluster of boulders occurs at the foot of the hillslope talus, but isolated boulders lie along the terrace well beyond these clusters. The boulders are mostly locally derived but there are scattered Palmer Land granite boulders with a axes of ~1 m. Pebbles are angular to sub-angular, with very few or no well-rounded pebbles. The gravel component includes striated clasts in gravel counts. Palmer Land erratics make up ~6% of clast content in stone counts, which is similar to the amounts of far-travelled material identified in the modern ice-cored ice-shelf moraines (Fig. 8). Towards the head of Ablation Valley, the terrace becomes increasingly less well-defined and buried by active scree slopes, though granite boulders continue to be visible. Three boulders from this terrace were sampled for cosmogenic nuclide dating.

4.4.3. Erratic Valley

In Erratic Valley, the drift with Palmer Land erratics comprises a cluster of local Alexander Island lithologies and granite, quartzite and gneiss boulders from Palmer Land lying directly on brecciated sandstone bedrock at elevations of 74–95 m asl, above the local valley glacier lateral moraines (Fig. 10; Fig. 13; Fig. 14A and B). Below this elevation, the Drift with Palmer Land erratics is overlain by degraded and fresh, ice-cored valley glacier lateral moraines.

At the foot of Erratic Valley, a wide ridge, 5–8 m asl, is well exposed, where it cuts across older valley glacier lateral moraines at the foot of the valley. The prominent ridge is littered with >35 Palmer Land erratic boulders, including granite, gneiss, diorite and

psammite (Fig. 13; Fig. 14D). This was dated with boulder sample L12.244. Beyond this lies fresh, ice-cored, ice-shelf moraine. A small epishelf lake is dammed directly in front of Erratic Glacier.

4.4.4. Moutonnée Valley

In Moutonnée Valley, striated bedrock (orientated at 291° , with plucked northern and eastern faces) and roches moutonnées are overprinted by the Drift with Palmer Land erratics up to 140 m asl. A silty diamicton with a lag of pebbles and cobbles, including granites (10% in stone counts), rests on a small knoll of striated bedrock at this elevation. Boulder L12.249 was sampled for cosmogenic nuclide dating here (Fig. 10). At 85 m asl in Moutonnée Valley, an undulating featureless slope with discontinuous ridges and benches is covered with a sandy gravel with 17% Palmer Land erratics (Fig. 5). Granite cobbles and small boulders occur all the way up the slope to this point. On the southern margin of Moutonnée Valley, a series of benches were observed between 9 and 30 m asl, but they are overprinted with scree and angular boulders derived from local rockfall. Granite boulders were mapped along these benches (Fig. 5).

Within Moutonnée Valley, there are several benches on the side of the valley littered with Palmer Land erratics. Boulder sample L12.247 (18 m asl) was sampled for cosmogenic nuclide dating from a wide, smooth slope on the northern side of the valley, dipping at $<5^\circ$ towards the lake. This is inferred to be equivalent to the 15–20 m terrace in Ablation Valley. The slope is scattered with large boulders, with a range of local and exotic lithologies present.

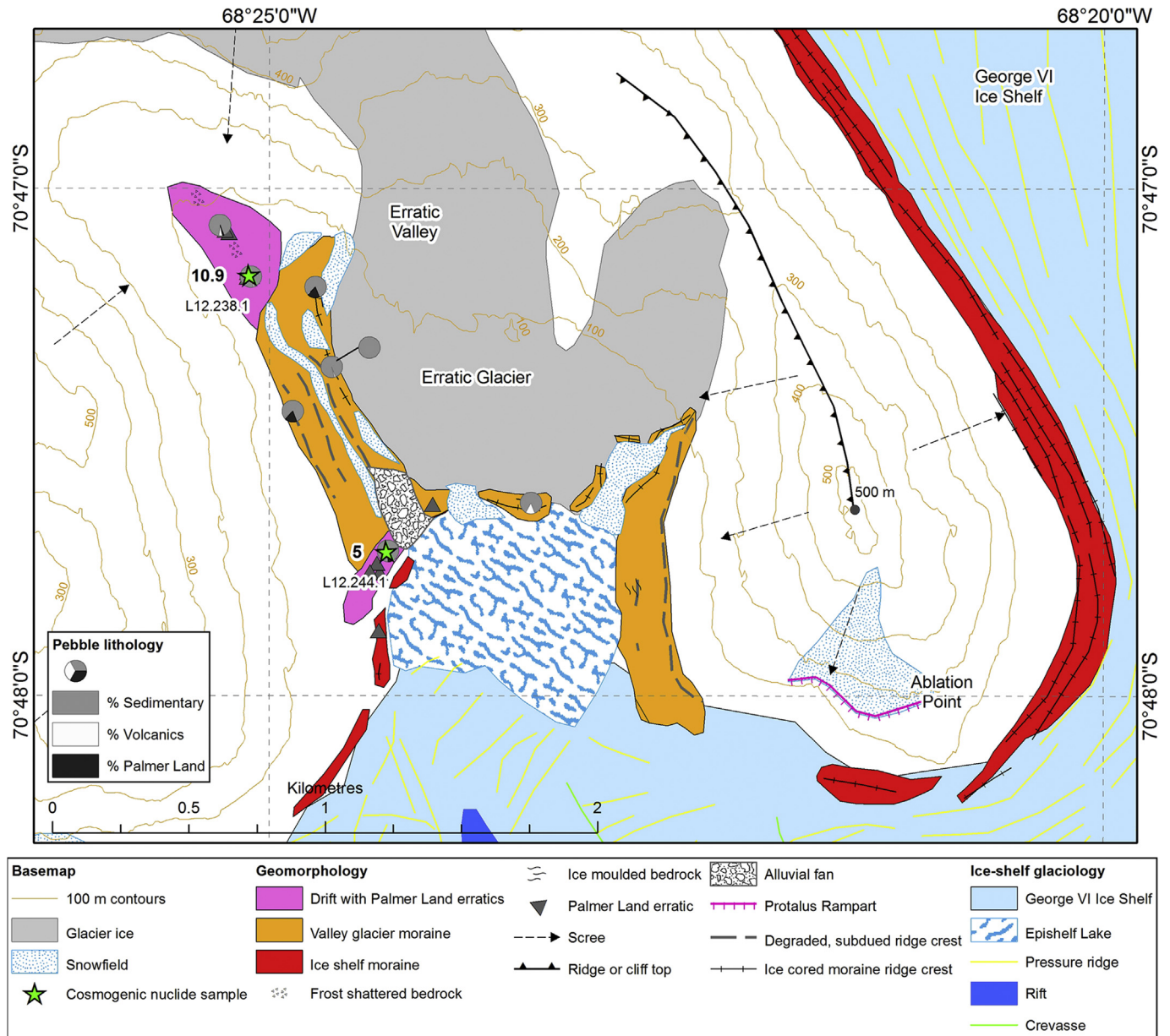


Fig. 13. Detailed geomorphological map of Erratic Valley, showing the complex relationship between the Drift with Palmer Land Erratics, subdued and degraded valley glacier moraine and modern, ice-cored ice-shelf moraines and valley glacier moraines.

Benches were also observed contouring around the hillside at 10 m, 12 m, and 25 m. These benches are associated with a silty to diamictic matrix with Palmer Land erratic. Correlative benches at the same altitude bearing granite erratics were also observed on the southern side of the valley.

A rocky spit of weathered basaltic bedrock (16 m asl) bars part of Moutonnée Lake (Fig. 4F). Here, a pebble lag overlies a clast-rich muddy diamicton with numerous granite cobbles. A granite boulder (L12.245) was sampled here for cosmogenic nuclide dating.

4.4.5. Interpretation

There are several mechanisms by which granite erratics could be distributed to heights of up to, but not above, 140 m asl in the inner valleys. Firstly, they could have been distributed by the LGM ice flowing from the Antarctic Peninsula over Alexander Island. However, this would require the direction of ice flow to be contrary to

the currently accepted view that ice was centred in and flowed into and along George VI Sound (cf. Fig. 1, with transverse flow from the margins), with an ice divide along the mountain range on Alexander Island. So this mechanism is unlikely. Secondly, these landforms have previously been interpreted as palaeo ice-shelf moraines (Clapperton and Sugden, 1982, 1983). However, this would require Holocene sea levels to be an order of magnitude higher than the currently recognised marine limit of 21.7 m (Simkins et al., 2013). This was revised down from an earlier study, which suggested that the Holocene marine limit in this area was 41 m asl at around 9000 ^{14}C years BP (Bentley et al., 2005a). Even accounting for ice-shelf thickening, it is difficult to explain the highest drift with Palmer Land Erratics, up to 100 m above this level, as being deposited by a floating ice shelf. To deposit high elevation erratics, the ice shelf would need to have a freeboard of around 100 m. Given the depth of the fjord reaching only 890 m

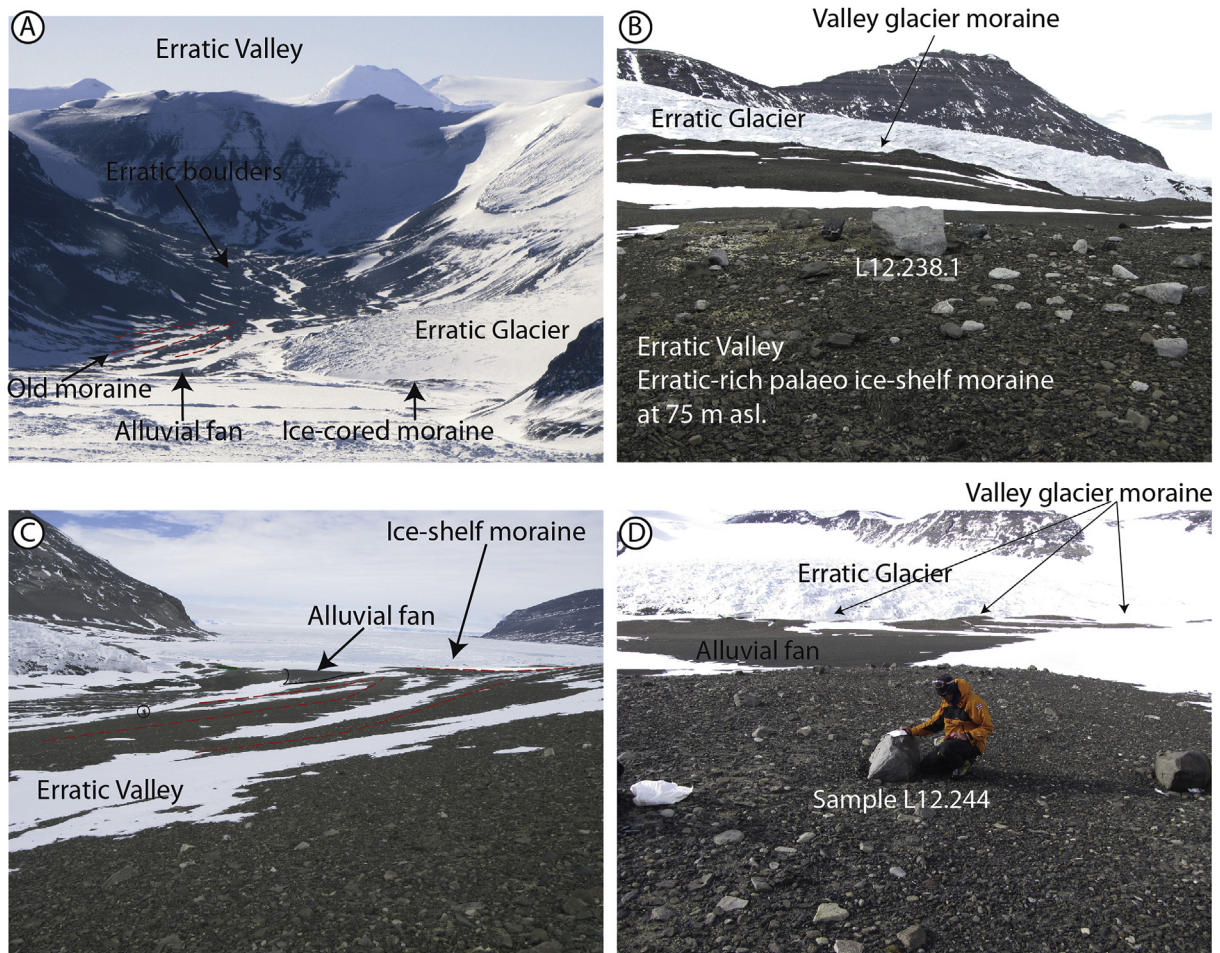


Fig. 14. Photographs of Erratic Valley. A. Erratic Valley, showing the older, degraded valley glacier moraines. Drift with Palmer Land erratics lies above these. B. Palmer Land granite boulders at high elevations (80 m asl) in Erratic Valley. C. Degraded valley glacier moraine overlain by fresh, ice-cored ice-shelf moraine (5–8 m asl) at the foot of Erratic Valley. Person circled for scale. D. The youngest facies, the 5–8 m asl ridge at the foot of Erratic Valley. This ridge bears numerous Palmer Land erratics and cuts across the valley glacier moraines.

below sea level at its deepest at Ablation Point Massif, the ice would need to be grounded.

Rather, we interpret the ridges bearing Palmer Land erratics above our basecamp, at the eastern margin of Alexander Island, to be lateral moraines constraining the maximum thickness of Marguerite Trough Ice Stream. Around Ablation Point Massif, George VI Sound is 890 m deep (Fretwell et al., 2013), meaning that lateral moraines at 120 m asl give an ice thickness of ~1030 m at this time. This is similar to the thickness of Marguerite Trough Ice Stream in this location predicted from numerical models (Colledge et al., 2012; Jamieson et al., 2012), and similar to the ‘typical’ ice thickness suggested by Truffer and Echelmeyer (2003).

Ridges previously interpreted as palaeo ice-shelf moraines can be traced all along the eastern margin of Alexander Island at this elevation (Clapperton and Sugden, 1982, 1983). We suggest that these ridges could all represent the lateral margins of Marguerite Trough Ice Stream. Similar features, interpreted as lateral moraines from an ice stream within a deep sound, have been observed on James Ross Island, northern Antarctic Peninsula (Glasser et al., 2014).

In the inner valleys at Ablation Point Massif, the drift with Palmer Land erratics (up to 140 m asl) comprises scattered granite and quartz diorite erratics, surficial sediments with a silty to diamictic composition, and subtle, indistinct, cross-valley discontinuous benches and ridges. In places, such as Erratic Valley,

accumulations of granite erratic boulders are found directly on brecciated bedrock. Longitudinal stresses, membrane stresses and local pinning points mean that the ice stream would be unlikely to penetrate deeply into the narrow, inner valleys. However, a grounded ice stream in George VI Sound could trap lateral lakes against the high ground. We propose that the series of benches with granite erratics, superimposed on the hillside on the eastern margin of Alexander Island within the inner valleys, represent palaeo shorelines from ice-dammed lakes. The similarity in their textural composition to the modern, ice-cored, ice-shelf moraines (Fig. 10; Fig. 11) is due to the ice stream having a similar ice-flow pathway to the modern George VI Ice Shelf, and due to the delivery of glacially transported erratic boulders and cobbles to Ablation Point Massif in both cases. As has been noted in other ice-free areas on the Antarctic Peninsula (e.g., Davies et al., 2013), deflation of fines means that the pebbles and cobbles form a lag, below which is the fine-grained matrix.

A lake-ice conveyor has previously been suggested as a mechanism by which far-travelled material could be transported across an ice-dammed lake, from a calving margin to the far shore (Hendy et al., 2000). Palaeo-conveyor deposits observed elsewhere in Antarctica comprise cross-valley and longitudinal ridges and sediment mounds (Hall et al., 2006). Where the lake level remains stable for some time, a shoreline with glacially transported and local debris may form. Where the lake level changes rapidly, coarse

debris is strewn across the hillside in a series of discontinuous mounds and ridges, scattered with boulders (Hall et al., 2006), such as that observed in the inner valleys at Ablation Point Massif. Variation occurs due to changes in sediment supply, stability of the lake level, and length of time involved. Sediments deposited by palaeo lake-ice conveyors typically comprise silts coarsening upwards into poorly sorted debris, with gravels and boulders that can exceed 3 m in diameter (Hall et al., 2006). Concentrations and mounds of sediment, such as that seen at 75–90 m asl in Erratic Valley, where there are numerous large Palmer Land boulders, may represent debris released from the base of icebergs trapped in the lake ice (termed *grounding line mounds*; Hendy et al., 2000; Hall et al., 2006). The narrow valleys would funnel icebergs trapped in the lake ice to form accumulations of boulders at high elevations, such as those observed in Moutonnée Valley and Erratic Valley.

We therefore interpret the drift with Palmer Land erratics in the inner valleys above the height of the 15–20 m terrace, as representing an ice-dammed lake, with an active lake-ice conveyor transporting material from the ice shelf to the inner valleys. However, lithologically the drift with Palmer Land erratics is very similar throughout its distribution, and discriminating between epishelf lake moraines and ice-shelf moraines is challenging. Local valley glaciers on Alexander Island may have flowed into the lake, but much of the area was ice-free at this time, leaving the shorelines preserved until the present day.

The prominent 15–20 m terrace extending along the southern margin of Ablation Valley and along Moutonnée Valley is interpreted as a palaeo-lake shoreline from a stable, persistent, higher-elevation epishelf lake, presumably formed during a period with a higher ice-shelf surface. This is supported by the presence of terraces with smooth slopes and littered with Palmer Land erratics occurring at a consistent height across two valleys. Wave action is limited in ice-covered lakes, especially given the short fetch at Ablation Point Massif, which limits typical beach features such as cobble imbrication and edge-rounding. Saturation and slumping of unconsolidated sediments from steep valley walls can result in the development of such terraces (Hendy et al., 2000), and stable lake levels can mean a lake-ice conveyor deposits material over a long period of time, building a longitudinal ridge enriched with glacially derived material (cf. Hall et al., 2006). Epishelf lakes are likely to form close to sea level, due to the hydraulic connection to marine waters. Independent studies confirm Holocene sea level reached this altitude (Simkins et al., 2013).

At the foot of Erratic Valley, a wide, prominent ridge at 5–8 m asl is interpreted as a palaeo ice-shelf moraine. This is due to its distinct ridge morphology, which contrasts with the flatter terraces observed in association with epishelf lake palaeo shorelines. It lies 100 m away from a fresh, sharp-crested, ice-cored ridge rich in Palmer Land erratics interpreted as a more recent ice-shelf moraine. The present-day ice shelf lies just beyond this ice-shelf moraine.

4.5. Valley glacier moraines

The local valley glaciers around Ablation Point Massif are characterised by steep terminal faces with little entrained glacial debris. Some supraglacial meltwater processes were evident, with frozen waterfalls originating from the glacier surface at the margin. The ice margin of Ablation Glacier is degraded into pinnacles and gullies. The glaciers of Ablation Point Massif generally have older, outer moraines, characterised by a subdued form and angular local pebbles. Inside these there are chaotic and nested fresh, younger valley glacier moraines, with sharp-crested, ice-cored ridges (Fig. 15A and B) and mostly local pebbles with few or no striations or facets. The sharp-crested moraines are interrupted by circular

depressions, interpreted as kettle holes. The ridge crests denote the incursion of several glaciers into the moraine complex (Fig. 15A). Lateral meltwater channels are incised through older moraines of Ablation Glacier (Fig. 15A).

In the valley glacier moraines, clast shape tends towards elongated blocks, and clasts are typically very angular (Fig. 16). The matrix texture is uniformly coarse, poorly sorted gravel, entirely different to the silty to diamictic textural variety associated with the drift with Palmer Land erratics. Above “The Mound”, lateral moraines impinge and flow around the top of the hill. The ice here is scattered with supraglacial boulders derived from the cliffs directly up-ice. The valley glacier moraines show a distinct lithological difference to the lithologies found in the modern ice-shelf moraines and drift with Palmer Land erratics (Fig. 11; Fig. 16). They are dominated by sandstones (e.g., L12.236, L12.253) and basaltic lavas from the Fossil Bluff Group (e.g., L12.243) (Supplementary Table 1).

At the head of Ablation Valley and in Erratic Valley, outer valley glacier lateral moraines overlie the palaeo lake shorelines with Palmer Land erratics (Fig. 14); in these lateral moraines, there are rare Palmer Land erratics reworked by the glacier into the moraine clast assemblage (Fig. 13). The inner lateral moraines of Erratic Glacier are characterised by lines of clast-supported boulders; they occur both along moraine ridge crests but also in the absence of a definable, clear ridge crest (Fig. 15C). The boulders lack polish, striations or edge-rounding. Ice-cored debris cones, up to 8 m high, are also located in the lateral margin of Erratic Glacier.

At the bottom of Erratic Valley, these valley glacier lateral moraines are in turn overprinted by the 5–8 m palaeo ice-shelf moraine. Beyond this lie younger, ice-cored and sharp-crested ice-shelf moraines (Fig. 13). Finally, the most recent expansion of the valley glaciers at Ablation Point Massif is recorded by fresh, sharp-crested, ice-cored valley glacier moraines. These moraines are characterised by angular pebbles, a lack of fine-grained material and Alexander Island pebbles only. In Erratic Valley, these fresh ice-cored valley glacier moraines cross-cut the 5–8 m a.s.l. palaeo ice-shelf moraine near the glacier terminus (Fig. 13).

The pinnacles and gullies of the glacier snout are similar to those observed on cold-based glaciers in the Dry Valleys, where differential ablation due to the presence of foliation and wind-blown sand results in a degraded ice surface (Hambrey and Fitzsimons, 2010). The angular nature of the clasts within these valley glacier moraines suggests that the glaciers that produced them were slow moving, with little erosive power (cf. Glasser and Hambrey, 2001; Hambrey and Ehrmann, 2004; Hambrey et al., 2005; Hambrey and Glasser, 2012). The low density of striations and faceting on the clasts is suggestive of limited basal sliding. “Boulder-belt” moraines, buried ice and ice-cored debris cones are also typical of Antarctic cold-based glaciers. “Boulder-belt” moraines are associated with the passive release of debris from the stationary margin of a slow moving glacier (Atkins, 2013). Lateral meltwater channels have previously been described for cold-based glaciers in the Dry Valleys (Atkins and Dickinson, 2007; Lloyd Davies et al., 2009). The thermal regime of these glaciers is therefore likely to be cold based, which is in line with their small size and the cool climate of Alexander Island. This contrasts with the more faceted, more frequently striated, and less angular clasts (particularly the far-travelled component) found within the palaeo and present-day ice-shelf moraine.

5. Chronology

Cosmogenic nuclide ages are presented in Table 1 and Fig. 5. Full sample details are presented in Supplementary Information. 21 samples were analysed for ^{10}Be and ^{26}Al . Of these, eight samples

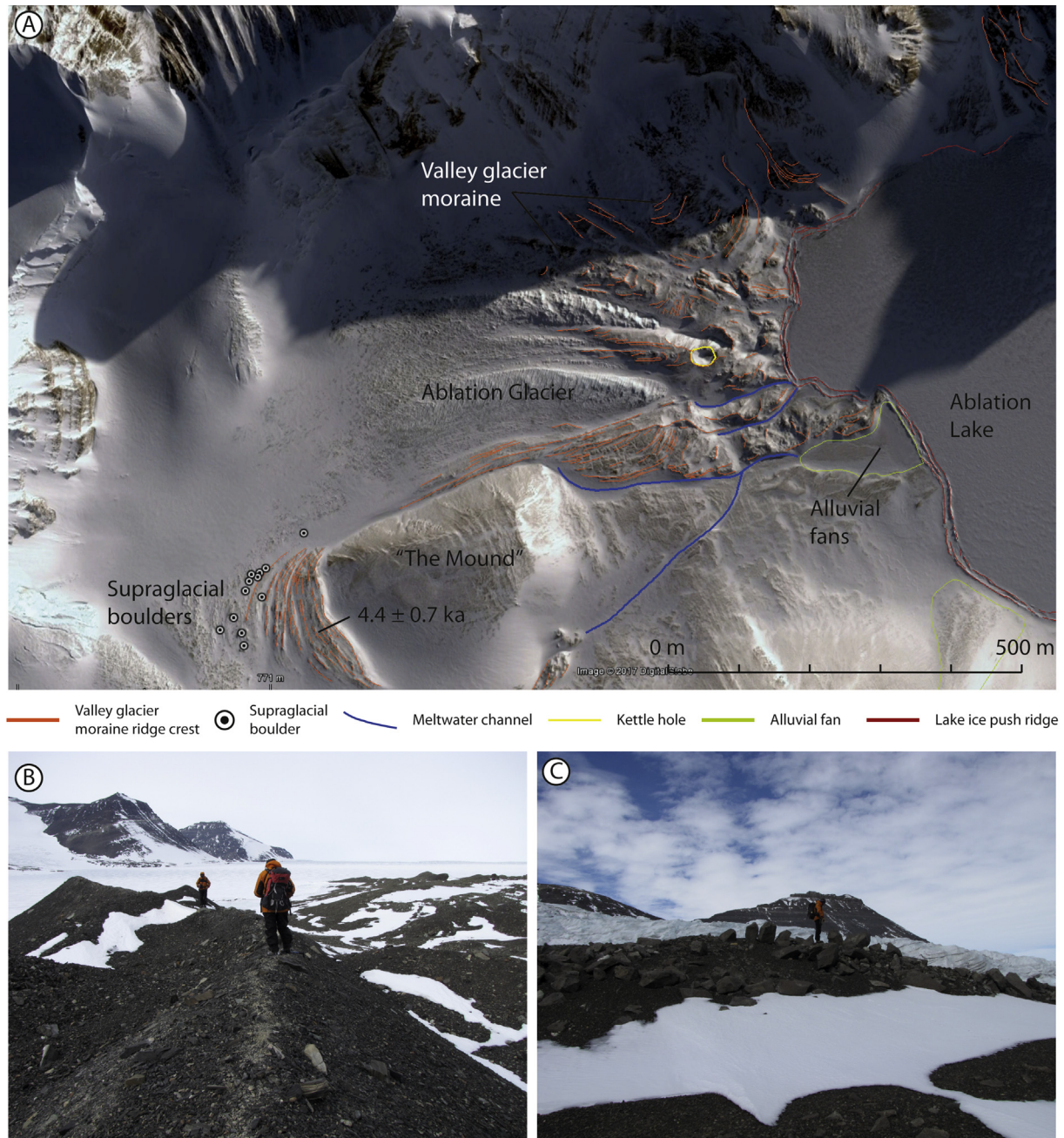


Fig. 15. A. Digital Globe image from Google Earth Pro showing Ablation Glacier. Brown lines denote moraine ridge crests; meltwater channels in blue; kettle holes in yellow; lake ice push ridges in red; alluvial fans in green. Cosmogenic nuclide sample L12.253.1 shown. B. Sharp-crested ice-cored moraines around Ablation Valley glacier. C. Lines of boulders on ridge crests, lateral moraine of Erratic Glacier. (For interpretation of the references to colour in this figure legend, the reader is referred to the web version of this article.)

failed to deliver meaningful results because of insufficient quartz content. Five samples had a very low ^{27}Al current, and the average scatter of the ^{26}Al ages is reported only for information purposes. In total, 15 ^{10}Be and 12 ^{26}Al cosmogenic nuclide ages are presented here for Ablation Point Massif (Fig. 17; Table 1). Considering the higher precision of the ^{10}Be measurements, and in order to facilitate the comparison with other published work in the region, we present all ages in the text as ^{10}Be ages.

Fig. 18A shows that ^{10}Be and ^{26}Al concentrations agree with the production rate ratio within errors, indicating that all the represented samples are compatible with a continuous exposure history. All samples overlap within a 1σ error of the erosion island (Supplementary Information) (as the $^{26}\text{Al}/^{10}\text{Be}$ sample ratios agree with

the production ratio, it is because they are “touching” the constant-exposure line of the banana plot, and they should yield the same apparent ages). The close agreement between the ^{26}Al and ^{10}Be ages ($r^2 = 0.98$; Fig. 18B) further supports the argument that these samples have all experienced a simple exposure. However, with samples this young, scatter on the banana plot (Supplementary Information) is likely to be the result of analytical uncertainty in the ^{26}Al analysis, rather than complex exposure.

In order to model the duration, start and end ages and possible outliers we developed a two-phase sequential model for the ages, constrained by our interpretation of the record as two separate periods of ice-shelf and ice-stream lake formation. This was used to develop our prior, along with the application of boundaries to

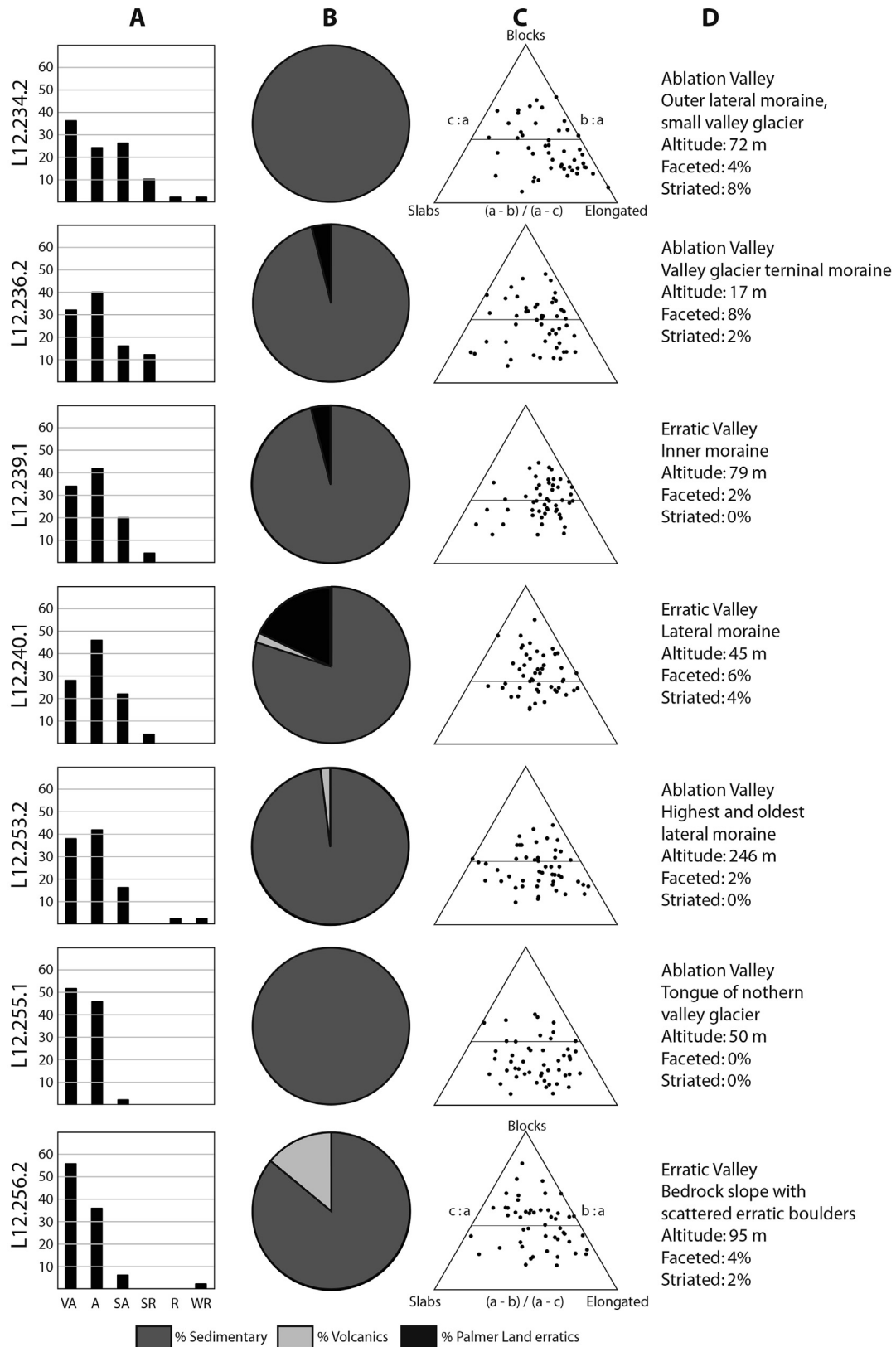
Valley glacier moraine (representative samples)

Fig. 16. Representative clast data from valley glacier moraines. Column A: Percentage clasts in each roundness category (Very Angular, Angular, Subangular, Subrounded, Rounded, Well rounded). Column B: Percentage clasts in different lithological categories (Sedimentary, Volcanics, Palmer Land erratics, and unknown). Column C: Clast shape ternary plots. Column D: Details of sample location and percentage of clasts that are striated or faceted.

Table 1
The successful samples and internal uncertainties (one sigma) for Ablation Point Massif. Full sample details are presented in Supplementary Information. Results are also shown in Figs. 5, 13, 17 and 18. *Outlier, excluded from further analysis.

| Lithofacies | Sample ID | Latitude | Longitude | Altitude (m asl) | Location | % Palmer Land erratics | ¹⁰ Be years | ²⁶ Al years |
|-------------------------------------------------------|-----------|------------|------------|------------------|----------------------------------------|------------------------|------------------------|------------------------|
| Ice stream lateral moraines | L12.225.1 | −70.83823 | −68.367491 | 120 | South of Ablation Lake | 10% | 17173 ± 1844 | — |
| | L12.224.4 | −70.83886 | −68.364344 | 116 | South of Ablation Lake | 18% | 3813 ± 531* | 4141 ± 554* |
| Marguerite Trough Ice Stream lateral ice-dammed lakes | L12.249.1 | −70.860072 | −68.392376 | 140 | Moutonnée Valley | 10% | 13877 ± 1358 | 13850 ± 1618 |
| | L12.216.1 | −70.820805 | −68.510279 | 90 | Head of Ablation Valley | 20% | 9681 ± 996 | 11349 ± 1240 |
| | L12.238.1 | −70.786215 | −68.418613 | 75 | Erratic Valley | 0% | 10878 ± 1129 | 11533 ± 1198 |
| | L12.232.1 | −70.821665 | −68.501756 | 69 | Head of Ablation Valley | 10% | 20596 ± 2025 | 20083 ± 2032 |
| | L12.231.1 | −70.820827 | −68.489606 | 31 | Head of Ablation Valley | 18% | 3757 ± 604* | — |
| GVIIS palaeo epishelf lake shoreline | L12.226.1 | −70.8443 | −68.333654 | 22 | Eastern Ablation Valley | 10% | 7950 ± 808 | 8623 ± 921 |
| | L12.202.2 | −70.827117 | −68.429817 | 14 | South shore of Ablation Lake | 2% | 9412 ± 998 | 9409 ± 1031 |
| | L12.206.1 | −70.839931 | −68.344665 | 15 | South shore of Ablation Lake | 30% | 6468 ± 682 | 6685 ± 743 |
| | L12.247.1 | −70.860984 | −68.349043 | 18 | Moutonnée Valley | 2% | 6732 ± 794 | 5768 ± 704 |
| | L12.245.1 | −70.866666 | −68.315603 | 16 | Rock spit at Moutonnée Point | 0% | 8643 ± 917 | 9193 ± 1017 |
| | L12.215.1 | −70.820707 | −68.480487 | 12 | Lower terrace, head of Ablation Valley | 32% | 3096 ± 360 | 2919 ± 347 |
| Palaeo ice-shelf moraine | L12.244.1 | −70.7953 | −68.404893 | 8 | 5–8 m terrace, foot of Erratic Valley | 6% | 4995 ± 670 | 4569 ± 541 |
| Valley glacier moraine | L12.253.1 | −70.821905 | −68.535749 | 246 | Ablation Valley; above “The Mound” | 0% | 4432 ± 707 | — |

separate the start and end of the phases recorded and dated here. For a discussion of the application of phase modelling to geological records see Blockley et al. (2008) and Chiverrell et al. (2013).

As shown in Fig. 18C, there are two clear outliers with respect to the general deglaciation trend. An outlier detection model using OxCal (4.3; Bronk Ramsey (2009a)) suggested that samples L12.224.4 (116 m) and L12.231.1 (31 m) were outlying to 100% and 68% respectively in relation to the other ages and the chronological constraints of the model prior. The contribution of these ages to the overall model and the timing of the start and end boundaries were thus down-weighted proportionally. Sample L12.231.1 also had a poor ²⁶Al run. Outliers were detected using the general outlier model (Bronk Ramsey, 2009b) and a likelihood of 0.05 (95%) of any date not being outlying. We infer that these samples were rejuvenated by the presence of exhumation, overlying debris or block rotation. The phase model in Oxcal identified Phase 1 (Marguerite Trough Ice Stream lateral lakes) as having start age boundaries of 25935–11709, and an end age boundary of 11630–7854. Phase 2 (GVIIS epishelf lakes) had a start age boundary of 10368–7196, and an end age boundary of 8230–306 (Fig. 18D).

6. Discussion

6.1. Ice-stream dynamics

A revised and updated event stratigraphy from that presented by Smith et al. (2007a) and Clapperton and Sugden (Sugden and Clapperton, 1980; Clapperton and Sugden, 1982) can be constructed from the new data presented in this paper (Table 2). Maximum glaciation of Alexander Island, with ice confluent with Palmer Land ice in George VI Sound, is recorded during MIS 4d to 2, based on *Hiattella solida* shells with ages of c. 75,000 or 30,000–18,000 years (Sugden and Clapperton, 1980; Clapperton and Sugden, 1982). This full ice-cap glaciation occurred with an ice divide centred on Alexander Island. Ice flowed down Ablation Valley and Moutonnée Valley (where it striated and moulded the bedrock) and out into George VI Sound, where it contributed to Marguerite Trough Ice Stream. This phase of glaciation is represented by our Drift with Alexander Island erratics on “The Mound” in Ablation Valley and by the roches moutonnées and striations at 90–140 m asl in Moutonnée Valley. Deglaciation and thinning of Alexander Island Ice Cap is constrained by published ¹⁰Be ages from in Moutonnée Valley (Fig. 5), suggesting that ice-cap thinning

commenced from 30 ka (Bentley et al., 2006), with an ice-sheet thickness of 650 m at 25.5 ± 1.7 ka, 600 m at 17.3 ± 1.8 ka, and 500 m at 11.9 ± 0.5 ka.

The first expansion of Marguerite Trough Ice Stream is recorded by ice-stream lateral moraines at 120 m asl above our basecamp (sample L12.225.1; 17.2 ± 1.8 ka). This ice stream dammed an enlarged lake in the inner valleys, with Palmer Land erratics scattered on discontinuous benches across the landscape and associated with a silty matrix diamicton at elevations of up to 140 m in Moutonnée Valley, 90 m in Erratic Valley, and at 90 m at the head of Ablation Valley (Fig. 19A). The ages of these ice-dammed lakes include 13.9 ± 1.4 ka from Moutonnée Valley (140 m asl). At the head of Ablation Valley, key samples include L12.216.1 (90 m), which yielded an age of 9.7 ± 1.0 ka (Table 1). Sample L12.232.1 (69 m asl) yielded an age of 20.6 ± 2.0 ka. In Erratic Valley, a cosmogenic nuclide sample taken at 75 m (L12.238.1) (Fig. 13) yielded an age of 10.9 ± 1.1 ka. These ages suggest that Marguerite Trough Ice Stream was active in the area until 9.7 ± 1.0 ka.

These lateral moraines and ice-dammed lake shorelines are the first terrestrial ages constraining ice thickness and timing of the onset of Marguerite Trough Ice Stream. These ages suggest that this ice stream was a deglacial feature, with ice streaming occurring during a period of general ice thinning in the region (cf. Bentley et al., 2006). A similar situation has been observed on James Ross Island, northern Antarctic Peninsula (Glasser et al., 2014).

Marine radiocarbon ages from the continental shelf edge suggest that the ice stream was at the continental shelf edge at the LGM (Ó Cofaigh et al., 2005b; Ó Cofaigh et al., 2005a; Kilfeather et al., 2011), and was on the inner continental shelf after 14 ka (Fig. 1; Table 2). The ice stream was likely much thicker at Ablation Point Massif at this time, in order to reach the required surface slope and driving stress to reach the shelf break. Our oldest ages (20.6 ± 2.0 ka and 17.2 ± 0.8 ka) therefore likely contain some ¹⁰Be inheritance. However, our ages from 13.9 to 9.7 ka indicate that during deglaciation, the ice stream surface at Ablation Point Massif lowered to 140 m asl and deglaciation occurred rapidly, with recession from the mid to inner continental shelf after 14.4 ± 1.2 ka (Pope and Anderson, 1992). Our cosmogenic ages also fit with numerical model outputs, which suggest that the main phase of thinning of the ice stream occurred at c. 12–11 ka, with some precursor thinning happening slowly before that, with thinning completed by ca. 9 ka (Golledge et al., 2014).

If the ice margin is at the mid-continental shelf after c. 14 ka, our

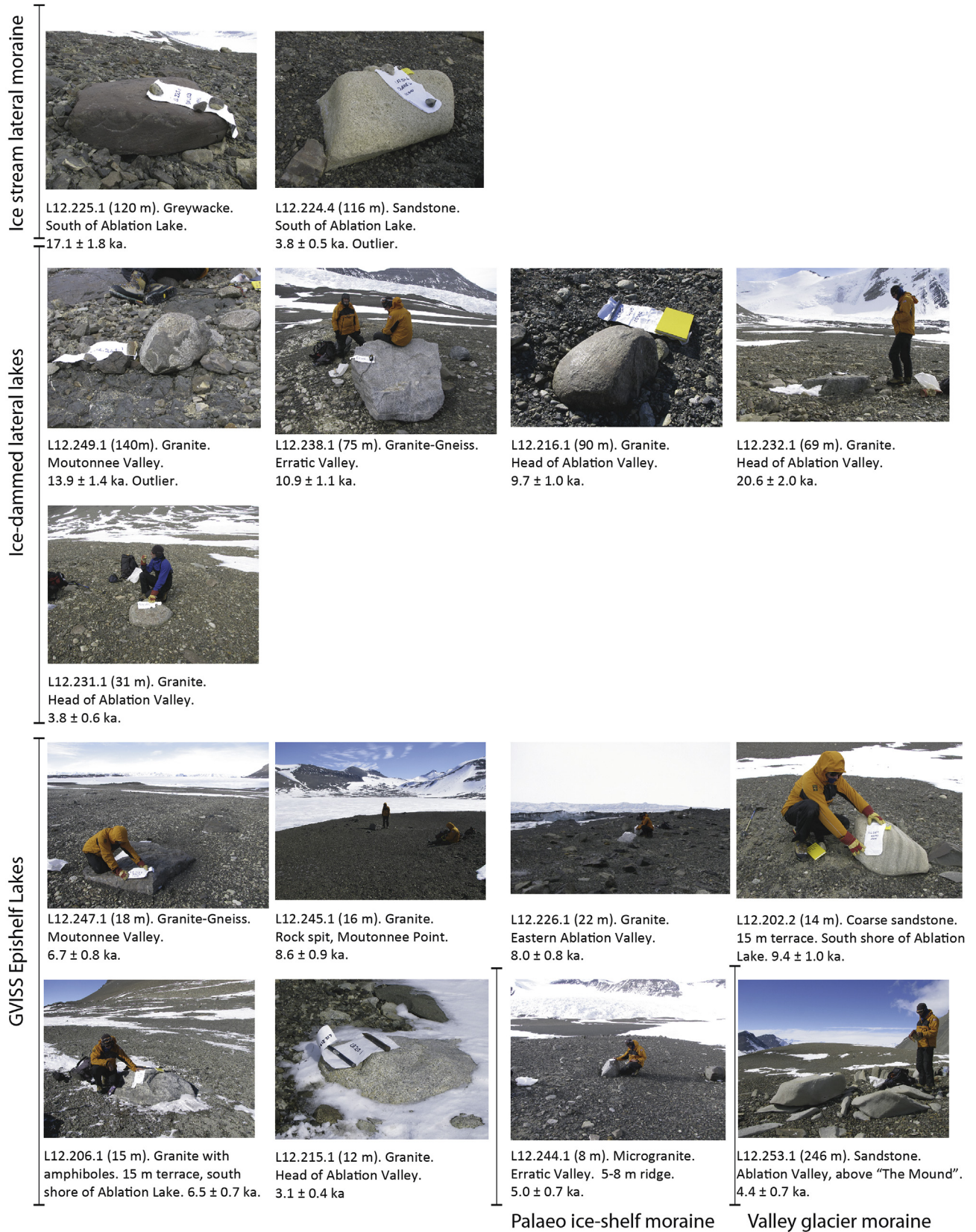


Fig. 17. Cosmogenic nuclide sample photographs from Ablation Point Massif.

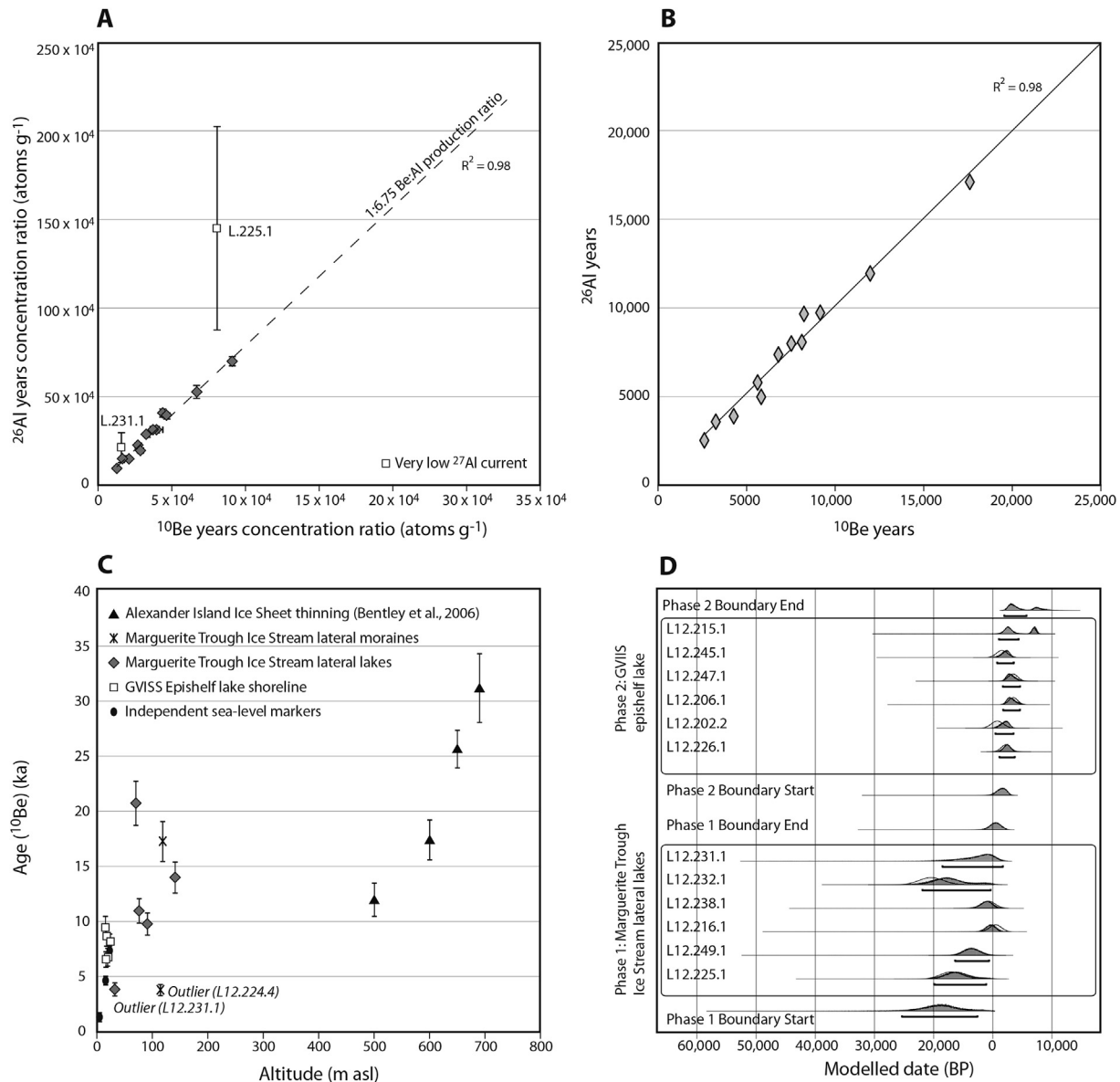


Fig. 18. A. Correlation of ^{10}Be and ^{26}Al concentrations for all samples with dual isotope analysis ($n = 15$). Error bars for internal uncertainties are shown; in most cases, error bars are smaller than data points. Dashed line indicates 1:6.75 Be:Al production ratio; most points plot along this line and show a strong correlation between ^{26}Al and ^{10}Be production ($r^2 = 0.98$), apart from three samples that have very low ^{27}Al currents and for which it was not possible to calculate a ^{26}Al exposure age. B. Correlation of ^{26}Al and ^{10}Be ages for all co-isotope samples ($n = 12$). C. Age-Altitude plot for samples from the samples at Ablation Point Massif. Published ^{10}Be ages from Bentley et al. (2006). Regional sea level indicators from published data (refs. Bentley et al., 2005b; Roberts et al., 2009; Simkins et al., 2013). This shows early thinning of the Alexander Island Ice Sheet, development of Marguerite Trough Ice Stream, with lateral moraines and lateral lakes, from 20.6 to 9.7 ka from 75 to 140 m asl, and development of the GVISS epishelf lake at 15–20 m asl at 9.4–4.6 ka. D. OxCal Bayesian phase model of ages in the two phases (GVISS epishelf lake and Marguerite Trough Ice Stream lateral lakes).

estimated ice thickness of 1030 m and an ice surface at 140 m asl from 13.9 to 9.7 ka gives a minimum ice-surface slope of 0.2° to 0.4° , depending on grounding line location. These values are lower than those we obtained from contemporary Antarctic ice streams from BEDMAP 2 data (Fretwell et al., 2013), which yield ice-surface slopes of $0.4^\circ - 0.6^\circ$ for the Siple Coast ice streams. Thwaites, Rutford and Institute ice streams have an ice-surface slope of 0.8° . Rydt et al. (2013) argue that typical values for ice stream mean surface slope is 0.003 rad (0.17°). Given the uncertainty in the grounding line position at the time of our ice-thickness reconstruction, we suggest that these values indicate that ice surface slope would yield sufficient driving stress to form an ice stream in Marguerite Bay.

6.2. Epishelf lakes

Epishelf lakes maintain a surface close to sea level (Galton-Fenzi et al., 2012; Hamilton et al., 2017). We infer that local isostatic depression of Alexander Island following the LGM resulted in a high relative sea level and therefore a higher elevation ice shelf, recorded by the 15–20 m epishelf lake palaeo-shoreline in both Ablation and Moutonnée valley. A lake-ice conveyor operated throughout the lake's existence, delivering erratic Palmer Land boulders to the distal shoreline (Fig. 19B).

This shoreline is dated using the ages obtained from samples L12.202.2 (14 m; $9.4 \pm 1.0 \text{ ka}$), L12.226.1 (22 m; $8.0 \pm 0.8 \text{ ka}$), L12.206.1 (15 m; $6.5 \pm 0.7 \text{ ka}$) and L12.247.1 (in Moutonnée Valley;

Table 2Event stratigraphy from Ablation Point Massif. Italics denote ages that likely contain ^{10}Be inheritance.

| Reference | Sample ID | Age (ka) | Uncertainty | Elevation (m asl) | Distance from sample site (km) | Facies interpretation | Significance |
|---------------------------------------------------------------------------------------------------------------|-------------|-------------------|-------------|-------------------|--------------------------------|--------------------------------------------------------------------------------------------------------------------------------------------------------------------------------|-------------------------------------------------------------------------|
| 1. Alexander Island Ice-Sheet thinning | | | | | | | |
| Bentley et al. (2006) | ABL 2 | 31 | 3.1 | 690 | | Alexander Island ice sheet | Old date above trimline Ice-sheet thinning |
| Bentley et al. (2006) | MV 2 | 25.5 | 1.7 | 650 | | | |
| Bentley et al. (2006) | MV 1 | 17.3 | 1.8 | 600 | | | |
| Bentley et al. (2006) | MV 3 | 11.9 | 1.5 | 500 | | | |
| 2. Recession of Marguerite Trough Ice Stream (see Fig. 1). Ages recalibrated in Ó Cofaigh et al., 2014 | | | | | | | |
| Pope and Anderson (1992) | PD88-99 | 14.4 | 1.2 | sea floor | 364 km | Transitional glaciomarine | Ice stream recession (minimum ages) |
| Kilfeather et al. (2011) | SUERC-23756 | 14.2 | 0.8 | sea floor | 389 km | | |
| Kilfeather et al. (2011) | SUERC-23755 | 14 | 0.6 | sea floor | 317 km | | |
| Ó Cofaigh et al. (2005a; 2005b) | VC307 | 10.4 | 0.4 | sea floor | 413 km | | |
| 3. Thinning of Marguerite Trough Ice Stream (Ablation Point Massif) | | | | | | | |
| This paper | L12.225.1 | 17.2 | 1.8 | 120 | | Lateral moraine for ice stream Ice-dammed lake, Moutonnee Valley Ice-dammed lake, Ablation Valley Ice-dammed lake, Erratic Valley Ice-dammed lake, Ablation Valley | Marguerite Trough Ice Stream |
| This paper | L12.249.1 | 13.9 | 1.4 | 140 | | | |
| This paper | L12.216.1 | 9.7 | 1.0 | 90 | | | |
| This paper | L12.238.1 | 10.9 | 1.1 | 75 | | | |
| This paper | L12.232.1 | 20.6 | 2.0 | 69 | | | |
| 4. Development of GV Ice Shelf and development of epishelf lakes in Ablation Point Massif | | | | | | | |
| This paper | L12.226.1 | 8.0 | 0.8 | 22 | | Epishelf lake (GVIIS) Epishelf lake (GVIIS) Rock spit, Moutonnée Lake Epishelf lake (GVIIS) Epishelf lake (GVIIS) | 15 m epishelf lake shoreline |
| This paper | L12.247.1 | 6.7 | 0.8 | 18 | | | |
| This paper | L12.245.1 | 8.6 | 0.9 | 16 | | | |
| This paper | L12.206.1 | 6.5 | 0.7 | 15 | | | |
| This paper | L12.202.2 | 9.4 | 1.0 | 14 | | Delta into lake Regional Holocene marine limit | Calmette Bay |
| Roberts et al. (2009) | AB1 | 4.6 | 0.4 | 14.4 | | | |
| Simkins et al. (2013) | 5.7–7.3 ka | 7.3 | | 21.7 | | | |
| Incursions of marine water beneath George VI Ice Shelf | | | | | | | |
| Smith et al. (2007b) | | 9.6–7.7 cal. BP | | | | Marine waters flowing into Moutonnée Lake | Deeper, higher epishelf lake/ ice-shelf absence and marine embayment |
| 5. Readvance of valley glaciers | | | | | | | |
| This paper | L12.253.1 | 4.4 | 0.7 | 246 | | Valley glacier lateral moraine | Imprinted on “The Mound”. |
| Undated moraines overly 15 m epishelf lake shoreline | | | | | | | |
| 6. Lowering of GVISS epishelf lake | | | | | | | |
| This paper | L12.244.1 | 5.0 | 0.7 | 8 | | Palaeo ice shelf moraine, Erratic Valley | Overlies valley glacier moraine |
| This paper | L12.215.1 | 3.1 | 0.4 | 12 | | Epishelf lake (GVIIS) | 12 m epishelf lake shoreline |
| 7. Neoglacial readvance of valley glaciers | | | | | | | |
| Valley glacier moraines overprint 5–8 m palaeo ice-shelf moraine near glacier terminus | | | | | | Readvance of glaciers on James Ross Island Readvance of glaciers at Rothera | |
| Davies et al. (2014) | | ~1.0 | | 895 km | | | |
| Guglielmin et al. (2015) | | 617-317 cal ka BP | | 362 km | | | |
| 8. Epishelf lake level lowers to 5 m above sea level today (present-day lake) | | | | | | | |
| Wasell and Håkansson, 1992 | | 1.3 | 0.2 | 3.5 | 338 km | Sea level constraints at Horseshoe Island | |
| 9. Twentieth century glacier recession | | | | | | | |
| Glacier recession ongoing behind the moraines. | | | | | | Glacier recession in 20th Century on James Ross Island | |
| Carrivick et al., 2012 | | | | 895 km | | | |
| Davies et al., 2012 | | | | 800 km | | Twentieth Century Trinity Peninsula glacier recession. | |

18 m; 6.7 ± 0.8 ka). Sample L12.245.1 (16 m) was taken from the rocky moraine-covered bar that impounds Moutonnée Lake. This sample yielded an exposure age of 8.6 ± 0.9 ka, consistent with an epishelf lake existing around this altitude in both valleys for several thousand years. An OSL age on the delta in Ablation Valley yielded an age of 4.6 ± 0.4 ka at 14.4 m, and provides support for a higher palaeo epishelf lake until this time. Given the amplitude of the thrusts in the lake ice, these ages and altitudes suggest that both Ablation Lake and Moutonnée Lake formed around 9.4 ± 1.0 ka and

remained in their present configuration until 4.6 ± 0.4 ka, after which the lake levels began lowering. Thus this epishelf lake potentially existed at a stable elevation (15–20 m asl) for some 5000 years (9.4 to 4.6 ka) in Moutonnée Valley and Ablation Valley, resulting in the formation of a large and prominent lake shoreline. Raised beaches in Marguerite Bay agree that sea level was around this elevation at this time (21.7 m at 5.5 to 7.3 ka) (Simkins et al., 2013). A slightly lower lake (12 m asl) was extant until 3.1 ± 0.4 ka, after which presumably the lake achieved its present-day

b) Mid-Holocene shoreline (9.4 ± 1.0 to 4.6 ± 0.4 ka)

c) Present day

Fig. 19. Schematic figure illustrating the proposed hypothesis for the delivery of erratic boulders to high elevations within the inner valleys (modified after [Smith et al., 2006a](#)). A: Marguerite Trough Ice Stream occupies George VI Sound, depositing lateral moraines along the margin of Alexander Island and damming lateral lakes in the inner valleys of Ablation Point Massif at elevations of up to 140 m. B: Marguerite Trough Ice Stream has receded and is replaced by George VI Ice Shelf. Epishelf lakes develop in Ablation and Moutonnée valleys. Higher sea levels result in the development of a stable, persistent lake for some 5000 years. Higher sea levels allow the advection of marine waters underneath the ice shelf. Basal erratics from Palmer Land were eroded from the bedrock on the Antarctic Peninsula by glaciers flowing into the ice shelf. They were then transported across George VI Sound in the ice shelf. C: Present-day. Local grounding and presence of a thick layer of fresh water means that marine influence is negligible.

configuration. Finally, the 5–8 m ice-shelf moraine in Erratic Valley is dated with sample L12.244.1 (8 m) (Fig. 13). This sample yields an age of 5.0 ± 0.7 ka.

The lake sediment record from Moutonnée Lake (sediment cores are marked on Fig. 19) suggests that at 9467 ± 30 ^{14}C years, waters bearing marine fauna first flowed into Moutonnée Lake (Smith et al., 2007b). We recalibrated these ages following the methodology outlined in Ó Cofaigh et al. (2014), using a marine correction of 1230 years and a ΔR of 830 ± 100 years. We obtained an age of 9.2 ± 0.4 cal ka BP for the first incursion of marine waters in Moutonnée Lake. The youngest age for marine fauna obtained was 8.2 ± 0.3 cal ka BP. An age of 7.7 cal ka BP was simply extrapolated by the original authors from the calculated sedimentation rate for the cessation of marine waters flowing into Moutonnée Lake.

Smith et al. (2007b) argued that, prior to the age of the oldest marine fauna (9.2 ± 0.4 cal ka BP), Moutonnée Lake existed in an epishelf environment similar to that of today (with the ice shelf being present), being perennially ice-covered, fresh-water dominated and largely unproductive (Smith et al., 2007b). There is no age control at the base of the lake core, so the period of deposition is uncertain. At 9.2 ± 0.4 cal ka BP, a marine biological assemblage is found in the core, along with higher abundances of clasts >8 mm (Roberts et al., 2008). The diatom assemblage is dominated by planktonic species, typically associated with pack-ice (Smith et al., 2007b). This assemblage is overlain by 1.87 m of unsorted gravel, potentially deposited rapidly as foraminiferal ages at the top and bottom of the unit are indistinguishable. This unit is overlain by a marine foraminiferal and diatom assemblage, though productivity declined towards the top of the marine section. The youngest age obtained is 8.2 ± 0.3 cal ka BP. The authors interpreted these data to suggest that George VI Ice Shelf was absent from Moutonnée Lake at this time (Smith et al., 2007b; Roberts et al., 2008). Smith et al. (2007b) argued that this was followed by re-isolation of the epishelf with a reversion back to current conditions, and a fresh-water dominated environment.

An alternative period of ice-shelf absence from 6850 to 6550 cal. yr BP, not recorded in the Moutonnée Lake cores, is suggested by the presence of reworked *Bathylasma* barnacles at the much higher elevation of 50 m asl at Two Steps Cliffs (cf. Hjort et al., 2001). However, these rare barnacles, which were not apparent at Ablation Point Massif, are reworked into the moraines and their exact provenance is uncertain.

Our ^{10}Be ages suggest that the ice shelf was stable and forming an epishelf lake at ~ 15 m asl Ablation Point Massif at this time. There are several hypotheses that could explain these conflicting data. The first is that our cosmogenic nuclide data simply do not record a brief period of ice-shelf absence (i.e., between 9.2 and 8.2 cal ka BP). Additionally, if the area became a marine embayment, then icebergs could raft boulders to the shorelines, in a similar manner to how icebergs have been observed around the coast of James Ross Island (Davies et al., 2013).

An alternative hypothesis could be that marine waters were able to flood underneath George VI Ice Shelf when its surface was at 15–20 m in the Moutonnée, Ablation and Erratic valleys (Fig. 19B). Sub ice-shelf marine waters in an ice shelf floating over a deep channel can include biogenic material advected from adjacent areas of seasonally open water (Pudsey and Evans, 2001), and sub ice-shelf sediments are likely to contain locally derived ice-rafted debris, due to the physical barrier of the ice shelf impeding icebergs. Riddle et al. (2007) summarised evidence of a marine biome existing today underneath GVIS, which includes foraminifera, diatoms and fish, supported by a food supply carried by currents. Hemer and Harris (2003) found open water diatom species in surface sediments taken from under Amery Ice Shelf, 80 km from open water. Hemer and Harris (2003) concluded that the presence

of marine organisms cannot be used as proof of corresponding open-water conditions. These factors could account for the biological assemblage and ice-rafted debris (Hambrey et al., 2015) found in sediment cores from Moutonnée Lake by Smith et al. (2007b).

In an epishelf lake setting, snow and ice meltwater from the catchment will accumulate in an epishelf lake until the thickness of the freshwater layer is equal to the minimum draft of the ice shelf (Hamilton et al., 2017). The excess of freshwater inflow is exported below the ice shelf to the open ocean. As the freshwater is limited to the draft of the ice shelf, an increasing marine influence and associated increasing foraminiferal and diatom assemblage would be expected at the base of the epishelf lake as the ice shelf surface raised and the lake became deeper. Conversely, a lowering of the ice shelf surface would result in decreasing marine influence and decreasing foraminifera and diatom assemblages, until the situation is reached, where similar to today, the lake is barren despite having a thin layer of saline marine waters at its base. Marine biota have been observed at the base of epishelf lakes in other settings (Vincent and Laybourn-Parry, 2008; Veillette et al., 2008).

The radiocarbon age of 9.2 cal ka BP from marine fauna within cores from Moutonnée Lake is consistent with the cosmogenic ages suggesting a 15–20 m ice-shelf surface during the early Holocene. During this period of higher sea levels, the increase in coarse clasts observed in the sediment cores from Moutonnée Lake (Roberts et al., 2008) could be derived simply from melt out from the base of the ice shelf, which presumably, with decreased grounding, penetrated further into the embayment than today. As the ice shelf would remain in contact with the shore of Alexander Island outside the limits of the Moutonnée Lake embayment, a mix of local and exotic clasts would be expected, as are observed in the ice-shelf moraines forming in this location today.

There is no evidence in our cosmogenic nuclide record for ice-shelf absence in this location from 9.2 to 8.2 cal ka BP (cf. Smith et al., 2007b). The ice-shelf collapse proposed by those authors also apparently occurred during a relatively cool period as recorded in the James Ross Island Ice Core, and was present during warmer periods from 5 to 3 ka and 12.6 to 9 ka. This is contrary to currently understood drivers and sensitivities of ice shelves to temperature (Morris and Vaughan, 2003; Cook and Vaughan, 2010). We therefore argue that the ice-shelf collapse hypothesised by Smith et al. (2007b) could be explained by marine waters circulating underneath the ice shelf and penetrating into Moutonnée Lake during a period of higher relative sea levels, according to independent measurements of sea level. Further work is required in order to establish the stability or otherwise of George VI Ice Shelf during the Holocene.

6.3. Valley glacier readvances

A Mid-Holocene readvance of the valley glaciers at Ablation Point Massif is recorded by subdued valley glacier moraines overlying the subdued ice-shelf moraine and truncating the 15 m terrace (Table 2). Our ^{10}Be age on the highest lateral moraine behind “The Mound” (Fig. 5; Fig. 15A) suggests that the maximum ice thickness was reached at 4.4 ± 0.7 ka (Sample L12.253.1). This may have occurred following the lowering of the ice shelf, changing the boundary conditions of the glaciers, or due to a regional climatic change. Data from James Ross Island Ice Core suggests that this was a period of relative warmth (Mulvaney et al., 2012). The 5–8 m ice-shelf moraine in Erratic Valley (5.0 ± 0.7 ka; Fig. 13) cuts across the valley glacier moraines and indicates that this glacier receded before this time. These ages are within errors of each other, suggesting that the readvance was short-lived. An increase in locally derived clast content observed in the Moutonnée Lake and

Ablation Lake cores (Smith et al., 2006b; Roberts et al., 2008) is consistent with increasing activity of valley glaciers at this time. As the cold-based glaciers today have large moraines, a readvance into the lake would increase delivery of glacially transported material to the bottom of the lake.

There are few instances of glacier advance around 5 ka recorded across the Antarctic Peninsula, when most other records suggest that glaciers were thinning and retreating (reviewed in Ó Cofaigh et al., 2014). The ice core record from James Ross Island suggests that this advance postdates a period of temperatures similar to present, and that the readvance ended during a period of warming (Mulvaney et al., 2012). This valley glacier readvance may therefore have been driven by a dynamic valley glacier response to ice-shelf retreat from Ablation Valley, or by increased precipitation.

A later, second readvance by the valley glaciers, resulting in sharp-crested, ice-cored moraines, post-dates this event with the deposition of terminal moraines truncating the ice-shelf moraines in Erratic Valley. This could be related to a Neoglacial readvance; a glacier readvance from 617 to 317 cal. yr BP has been recorded at Rothera Ramp, 360 km north of the study location (Guglielmin et al., 2015). An ice advance postdating 700–970 cal. yr BP is also recorded on Anvers Island (Hall et al., 2010). On James Ross Island, a glacial readvance with a maximum after ~1000 yr BP was also recorded (Davies et al., 2014). The James Ross Island Ice Core suggests that 1 ka was a period of strong regional cooling (Mulvaney et al., 2012; Abram et al., 2013), which may have driven the advance by limiting summer melt. Finally, the valley glaciers have receded behind these ice-cored valley glacier moraines, consistent with ongoing glacier recession across the Antarctic Peninsula (Smith et al., 1998; Cook et al., 2005; Davies et al., 2012; Carrivick et al., 2012).

7. Conclusions

In this study, we used geomorphological mapping, clast provenance and cosmogenic nuclide dating to reconstruct the history of Marguerite Trough Ice Stream and George VI Ice Shelf during the Holocene. Palaeo ice-shelf moraines and epishelf lake shorelines, deposited at the landward margin of the ice shelf on Alexander Island, contain a diverse and distinctive assemblage of lithologies from Alexander Island, as well as plutonic igneous rocks from Palmer Land. We provide one of the first detailed sediment-landform assemblage analyses for ice-dammed and epishelf lake sediments in this region, and contribute to the sparse but growing literature on these features.

Marguerite Trough Ice Stream reached up to 120 m asl in the vicinity of Ablation Point Massif. It imprinted lateral moraines all along the eastern coastline of Alexander Island, with similar landforms observed at Two Steps Cliffs at 110 m (Clapperton and Sugden, 1982; Smith et al., 2007a). The reconstructed ice stream had a thickness of around 1030 m. The ice stream formed after the LGM and remained during early deglaciation, with exposure ages of boulders on lateral moraines and on the shorelines of ice-dammed lakes yielding ages of 13.9 to 9.7 ka. These ages are consistent with the history of ice recession from radiocarbon ages on transitional glaciomarine sediments in Marguerite Trough. These are the first limits on Marguerite Trough Ice Stream ice thickness and the first terrestrial ages constraining ice stream dynamics.

An ice shelf formed in George VI Sound following recession of the Marguerite Trough Ice Stream. During a period of relatively high sea levels on Alexander Island, an epishelf lake dammed against George VI Ice Shelf at elevations of up to 15–20 m in Moutonnée Valley and Ablation Valley. This epishelf lake was stable for some 5000 years, existing continuously from 9.4 to 4.6 ka.

A period of ice-shelf collapsed was previously suggested from

9.2 ± 0.4 to 8.2 ± 0.3 cal ka BP (Smith et al., 2007b). However our data suggest that the epishelf lake existed continuously through this period of time. One explanation could be that during the early part of its formation, marine waters were advected underneath the ice shelf. Marine currents bearing foraminifera and diatoms deposited biota-rich sediments in these lakes. Rain-out from beneath the ice shelf deposited numerous gravel clasts within the lake basins. We find no unambiguous evidence that the ice shelf collapsed during the Holocene, but more work is required to further test this hypothesis.

We provide the first evidence of mid-Holocene valley glacier readvance, with moraines forming at 4.4 ± 0.7 ka. This valley glacier readvance occurred during a period of relative warmth as recorded in Antarctic Peninsula ice cores. The drivers of this glacier advance require further study, but they could be related to local climate or to a dynamic response to ice-shelf retreat from Ablation Valley and Erratic Valley. A final readvance occurred more recently, possibly during Neoglacial of cooling. During the Twentieth Century, the glaciers receded behind these Neoglacial moraines.

Acknowledgements

This project was funded by NERC grant NE/F012896/1 (*The Glacial History of the NE Antarctic Peninsula region over centennial to millennial timescales*), awarded to NFG (Principal Investigator) and MJH, JLS and JLC (co-investigators). BJD and MJH would like to thank the British Antarctic Survey for providing logistics, field access and equipment. Cosmogenic nuclide samples were funded through the NERC Cosmogenic Isotope Analysis Facility at the Scottish Universities Environmental Research Centre (CIAF award 9131/0413). BJD and MJH would like to thank Ian Hey for his excellent assistance in the field. We thank Nicholas Colledge (Antarctic Research Centre, Victoria University of Wellington) for helpful discussions comparing geological and numerical modelling data. We thank two anonymous reviewers for their constructive and insightful reviews, which did much to improve this paper.

Appendix A. Supplementary data

Further data supporting the article can be found in the Supplementary Information. This includes full cosmogenic nuclide sample details, full details of clast provenancing and thin section work, and Google Earth KML files for download and inspection.

Supplementary data related to this article can be found at <https://doi.org/10.1016/j.quascirev.2017.10.016>.

References

- Abram, N.J., Mulvaney, R., Wolff, E.W., Triest, J., Kipfstuhl, S., Trusel, L.D., Vimeux, F., Fleet, L., Arrowsmith, C., 2013. Acceleration of snow melt in an Antarctic Peninsula ice core during the Twentieth century. *Nat. Geosci.* 6, 404–411.
- Antoniades, D., Francus, P., Pienitz, R., St-Onge, G., Vincent, W.F., 2011. Holocene dynamics of the Arctic's largest ice shelf. *Proc. Natl. Acad. Sci. U. S. A.* 108, 18899–18904.
- Atkins, C., 2013. Geomorphological Evidence of Cold-based Glacier Activity in South Victoria Land, Antarctica, vol 381. Geological Society, London, Special Publications, pp. 299–318.
- Atkins, C.B., Dickinson, W.W., 2007. Landscape modification by meltwater channels at margins of cold-based glaciers, Dry Valleys, Antarctica. *Boreas* 36, 47–55.
- Balco, G., 2011. Contributions and unrealized potential contributions of cosmogenic-nuclide exposure dating to glacier chronology, 1990–2010. *Quat. Sci. Rev.* 30, 3–27.
- Balco, G., Stone, J.O., Lifton, N.A., Dunai, T.J., 2008. A complete and easily accessible means of calculating surface exposure ages or erosion rates from ^{10}Be and ^{26}Al measurements. *Quat. Geochronol.* 3, 174–195.
- Benn, D.I., 2007. Clast form analysis. In: Elias, S.A. (Ed.), *Encyclopedia of Quaternary Science*. Elsevier, Oxford, pp. 904–909.
- Benn, D.I., Ballantyne, C.K., 1994. Reconstructing the transport history of glacial sediments: a new approach based on the co-variance of clast form indices. *Sediment. Geol.* 91, 215–227.

- Bentley, M.J., 2010. The Antarctic palaeo record and its role in improving predictions of future Antarctic Ice Sheet change. *J. Quat. Sci.* 25, 5–18.
- Bentley, M.J., Fogwill, C.J., Kubnik, P.W., Sugden, D.E., 2006. Geomorphological evidence and cosmogenic $^{10}\text{Be}/^{26}\text{Al}$ exposure ages for the last glacial maximum and deglaciation of the Antarctic Peninsula ice sheet. *GSA Bull.* 118, 1149–1159.
- Bentley, M.J., Fogwill, C.J., Le Brocq, A.M., Hubbard, A.L., Sugden, D.E., Dunai, T.J., Freeman, S.P.H.T., 2010. Deglacial history of the west Antarctic ice sheet in the Weddell sea embayment: constraints on past ice volume change. *Geology* 38, 411–414.
- Bentley, M.J., Hodgson, D.A., Smith, J.A., Cox, N.J., 2005a. Relative sea level curves for the south Shetland Islands and Marguerite Bay, Antarctic Peninsula. *Quat. Sci. Rev.* 24, 1203–1216.
- Bentley, M.J., Hodgson, D.A., Sugden, D.E., Roberts, S.J., Smith, J.A., Leng, M.J., Bryant, C.L., 2005b. Early Holocene retreat of the George VI Ice Shelf, Antarctic Peninsula. *Geology* 33, 173–176.
- Berthier, E., Scambos, T., Schuman, C.A., 2012. Mass loss of Larsen B tributary glaciers (Antarctic Peninsula) unabated since 2002. *Geophys. Res. Lett.* 39, L13501.
- Bishop, J.F., Walton, J.L.W., 1981. Bottom melting under George VI Ice Shelf, Antarctica. *J. Glaciol.* 27, 429–447.
- Blockley, S.P., Bronk Ramsey, C., Pyle, D., 2008. Improved age modelling and high-precision age estimates of late Quaternary tephras, for accurate palaeoclimate reconstruction. *J. Volcanol. Geotherm. Res.* 177, 251–262.
- Bronk Ramsey, C., 2009a. Bayesian analysis of radiocarbon dates. *Radiocarbon* 51, 337–360.
- Bronk Ramsey, C., 2009b. Dealing with outliers and offsets in radiocarbon dating. *Radiocarbon* 51, 1023–1045.
- Burn, R.W., 1984. The Geology of the Lemay Group, Alexander Island. British Antarctic Survey, Cambridge.
- Butterworth, P., Crame, J., Howlett, P., Macdonald, D., 1988. Lithostratigraphy of upper jurassic-lower cretaceous strata of eastern Alexander Island, Antarctica. *Cretac. Res.* 9, 249–264.
- Carrivick, J.L., Davies, B.J., Glasser, N.F., Nývlt, D., Hambrey, M.J., 2012. Late Holocene changes in character and behaviour of land-terminating glaciers on James Ross Island, Antarctica. *J. Glaciol.* 58, 1176–1190.
- Chiverrell, R.C., Thrasher, I.M., Thomas, G.S., Lang, A., Scourse, J.D., van Landeghem, K.J., Mccarroll, D., Clark, C.D., Ó Cofaigh, C., Evans, D.J., 2013. Bayesian modelling the retreat of the Irish sea ice stream. *J. Quat. Sci.* 28, 200–209.
- Clapperton, C.M., Sugden, D.E., 1982. Late Quaternary glacial history of George VI Sound area, West Antarctica. *Quat. Res.* 18, 243–267.
- Clapperton, C.M., Sugden, D.E., 1983. Geomorphology of the Ablation Point Massif, Alexander Island, Antarctica. *Boreas* 12, 125–135.
- Cook, A.J., Fox, A.J., Vaughan, D.G., Ferrigno, J.G., 2005. Retreating glacier fronts on the Antarctic Peninsula over the past half-century. *Science* 308, 541–544.
- Cook, A.J., Vaughan, D.G., 2010. Overview of areal changes of the ice shelves on the Antarctic Peninsula over the past 50 years. *Cryosphere* 4, 77–98.
- Corbett, L.B., Young, N.E., Bierman, P.R., Briner, J.P., Neumann, T.A., Rood, D.H., Graly, J.A., 2011. Paired bedrock and boulder ^{10}Be concentrations resulting from early Holocene ice retreat near Jakobshavn Isfjord, western Greenland. *Quat. Sci. Rev.* 30, 1739–1749.
- Davies, B.J., Carrivick, J.L., Glasser, N.F., Hambrey, M.J., Smellie, J.L., 2012. Variable glacier response to atmospheric warming, northern Antarctic Peninsula, 1988–2009. *Cryosphere* 6, 1031–1048.
- Davies, B.J., Glasser, N.F., Carrivick, J.L., Hambrey, M.J., Smellie, J.L., Nývlt, D., 2013. Landscape evolution and ice-sheet behaviour in a semi-arid polar environment: James Ross Island, NE Antarctic Peninsula. In: Hambrey, M.J., Barker, P.F., Barrett, P.J., Bowman, V.C., Davies, B.J., Smellie, J.L., Tranter, M. (Eds.), *Antarctic Palaeoenvironments and Earth-surface Processes*, vol. 381. Geological Society, London, pp. 353–395. London, Special Publications.
- Davies, B.J., Gollidge, N.R., Glasser, N.F., Carrivick, J.L., Ligtnerberg, S.R.M., Barrand, N.E., van den Broeke, M.R., Hambrey, M.J., Smellie, J.L., 2014. Modelled glacier response to centennial temperature and precipitation trends on the Antarctic Peninsula. *Nat. Clim. Change* 4, 993–998.
- De Angelis, H., Skvarca, P., 2003. Glacier surge after ice shelf collapse. *Science* 299, 1560–1562.
- Doran, P.T., Wharton, R., Lyons, W., Des Marais, D., Andersen, D., 2000. Sedimentology and geochemistry of a perennially ice-covered epishelf lake in Bunger Hills Oasis, East Antarctica. *Antarct. Sci.* 12, 131–140.
- England, J.H., Furze, M.F., Doupe, J.P., 2009. Revision of the NW laurentide ice sheet: implications for paleoclimate, the northeast extremity of Beringia, and Arctic ocean sedimentation. *Quat. Sci. Rev.* 28, 1573–1596.
- Fretwell, L.O., Pritchard, H.D., Vaughan, D.G., Bamber, J.L., Barrand, N.E., Bell, R., Bianchi, C., Bingham, R.G., Blankenship, D.D., Casassa, G., Catania, G., Callens, D., Conway, H., Cook, A.J., Corr, H.F.J., Damaske, D., Damm, V., Ferraccioli, F., Forsberg, R., Fujita, S., Gogineni, P., Griggs, J.A., Hindmarsh, R.C.A., Holmlund, P., Holt, J.W., Jacobel, R.W., Jenkins, A., Jokat, W., Jordan, T., King, E.C., Kohler, J., Krabill, W., Riger-Kusk, M., Langley, K.A., Leitchenkov, G., Leuschen, C., Luyendyk, B.P., Matsuoka, K., Nogi, Y., Nost, O.A., Popov, S.V., Rignot, E., Rippin, D.M., Riviera, A., Roberts, J., Ross, N., Siegert, M.J., Smith, A.M., Steinhage, D., Studinger, M., Sun, B., Tinto, B.K., Welch, B.C., Young, D.A., Xiangbin, C., Zirizzotti, A., 2013. Bedmap2: improved ice bed, surface and thickness datasets for Antarctica. *Cryosphere* 7, 375–393.
- Galton-Fenzi, B.K., Hunter, J.R., Coleman, R., Young, N., 2012. A decade of change in the hydraulic connection between an Antarctic epishelf lake and the ocean. *J. Glaciol.* 58, 223–228.
- Glasser, N.F., Davies, B.J., Carrivick, J.L., Rodés, A., Hambrey, M.J., Smellie, J.L., Domack, E., 2014. Ice-stream initiation, duration and thinning on James Ross Island, northern Antarctic Peninsula. *Quat. Sci. Rev.* 86, 78–88.
- Glasser, N.F., Hambrey, M.J., 2001. Styles of sedimentation beneath Svalbard valley glaciers under changing dynamic and thermal regimes. *J. Geol. Soc. Lond.* 158, 697–707.
- Glasser, N.F., Kulesa, B., Luckman, A., Jansen, D., King, E.C., Sammonds, P.R., Scambos, T.A., Jezek, K.C., 2009. Surface structure and stability of the Larsen C Ice Shelf, Antarctic Peninsula. *J. Glaciol.* 55, 400–410.
- Glasser, N.F., Scambos, T.A., Bohlander, J.A., Truffer, M., Pettit, E.C., Davies, B.J., 2011. From ice-shelf tributary to tidewater glacier: continued rapid glacier recession, acceleration and thinning of Röhss Glacier following the 1995 collapse of the Prince Gustav Ice Shelf on the Antarctic Peninsula. *J. Glaciol.* 57, 397–406.
- Gollidge, N.R., Fogwill, C.J., Mackintosh, A.N., Buckley, K.M., 2012. Dynamics of the Last Glacial Maximum Antarctic ice-sheet and its response to ocean forcing. *Proc. Natl. Acad. Sci.* 106, 16052–16056.
- Gollidge, N.R., Menviel, L., Carter, L., Fogwill, C.J., England, M.H., Cortese, G., Levy, R.H., 2014. Antarctic contribution to meltwater pulse 1A from reduced Southern Ocean overturning. *Nat. Commun.* 5, 5107.
- Gosse, J.C., Phillips, F.M., 2001. Terrestrial in situ cosmogenic nuclides: theory and application. *Quat. Sci. Rev.* 20, 1475–1560.
- Graham, A.G.C., Smith, J.A., 2012. Palaeoglaciology of the Alexander Island ice cap, western Antarctic Peninsula, reconstructed from marine geophysical and core data. *Quat. Sci. Rev.* 35, 63–81.
- Guglielmin, M., Convey, P., Malfasi, F., Cannone, N., 2015. Glacial fluctuations since the 'Medieval Warm Period' at Rothera point (western Antarctic Peninsula). *Holocene* 26, 154–158.
- Hall, B.L., Hendy, C.H., Denton, G.H., 2006. Lake-ice conveyor deposits: geomorphology, sedimentology, and importance in reconstructing the glacial history of the Dry Valleys. *Geomorphology* 75, 143–156.
- Hall, B.L., Koffman, T., Denton, G.H., 2010. Reduced ice extent on the western Antarctic Peninsula at 700–970 cal. yr BP. *Geology* 38, 635–638.
- Hambrey, M.J., Davies, B.J., Glasser, N.F., Holt, T.O., Smellie, J.L., Carrivick, J.L., 2015. Structure and sedimentology of George VI Ice Shelf, Antarctic Peninsula: implications for ice-sheet dynamics and landform development. *J. Geol. Soc.* 172, 599–613.
- Hambrey, M.J., Ehrmann, W., 2004. Modification of sediment characteristics during glacial transport in high-alpine catchments: Mount Cook area, New Zealand. *Boreas* 33, 300–318.
- Hambrey, M.J., Fitzsimons, S.J., 2010. Development of sediment-landform associations at cold glacier margins, Dry Valleys, Antarctica. *Sedimentology* 57, 857–882.
- Hambrey, M.J., Glasser, N.F., 2003. The role of folding and foliation development in the genesis of Medial Moraine: examples from Svalbard glaciers. *J. Geol.* 111, 471–485.
- Hambrey, M.J., Glasser, N.F., 2012. Discriminating glacier thermal and dynamic regimes in the sedimentary record. *Sediment. Geol.* 251–252, 1–33.
- Hambrey, M.J., Murray, T., Glasser, N.F., Hubbard, A., Hubbard, B., Stuart, G., Hansen, S., Kohler, J., 2005. Structure and changing dynamics of a polythermal glacier on a centennial timescale: Midre Lovénbreen, Svalbard. *J. Geophys. Res.* 110, 1–19.
- Hamilton, A.K., Laval, B.E., Mueller, D.R., Vincent, W.F., Copland, L., 2017. Dynamic response of an Arctic epishelf lake to seasonal and long-term forcing: implications for ice shelf thickness. *Cryosphere Discuss* 2017, 1–34.
- Haran, T., Bohlander, J., Scambos, T., Painter, T., Fahnestock, M., 2014. MODIS Mosaic of Antarctica 2008–2009 (MOA2009) Image Map. National Snow and Ice Data Center, Boulder, Colorado USA. <https://doi.org/10.7265/N5KP8037>.
- Harangozo, S.A., Colwell, S.R., King, J.C., 1997. An analysis of a 34-year air temperature record from Fossil Bluff (71 S, 68 W), Antarctica. *Antarct. Sci.* 9, 355–363.
- Harden, S.L., DeMaster, D.J., Nittrouer, C.A., 1992. Developing sediment geochronologies for high-latitude continental shelf deposits: a radiochemical approach. *Mar. Geol.* 103, 69–97.
- Harris, J.S., Fleming, E.A., 1978. Northern Palmer Land, British Antarctic territory, geological map. Scale 1:500,000. Br. Antarct. Surv. (Cambridge).
- Hein, A.S., Marrero, S.M., Woodward, J., Dunning, S.A., Winter, K., Westoby, M.J., Freeman, S.P., Shanks, R.P., Sugden, D.E., 2016. Mid-Holocene pulse of thinning in the Weddell Sea sector of the West Antarctic ice sheet. *Nat. Commun.* 7.
- Hemer, M.A., Harris, P.T., 2003. Sediment core from beneath the Amery Ice Shelf, East Antarctica, suggests mid-Holocene ice-shelf retreat. *Geology* 31, 127–130.
- Hendy, C., Sadler, A., Denton, G., Hall, B., 2000. Proglacial lake-ice conveyors: a new mechanism for deposition of drift in polar environments. *Geogr. Ann. Ser. A, Phys. Geogr.* 82, 249–270.
- Heroy, D.C., Anderson, J.B., 2007. Radiocarbon constraints on Antarctic Peninsula ice sheet retreat following the last glacial maximum (LGM). *Quat. Sci. Rev.* 26, 3286–3297.
- Heywood, R., 1977. A limnological survey of the ablation point area, Alexander Island, Antarctica. *Philosophical Trans. R. Soc. Lond. B Biol. Sci.* 279, 39–54.
- Hillenbrand, C.-D., Larter, R.D., Dowdeswell, J.A., Ehrmann, W., Ó Cofaigh, C., Benetti, S., Graham, A.G.C., Grobe, H., 2010. The sedimentary legacy of a palaeo-ice stream on the shelf of the southern Bellingshausen Sea: clues to West Antarctic glacial history during the Late Quaternary. *Quat. Sci. Rev.* 29, 2741–2763.
- Hjort, C., Bentley, M.J., Ingólfsson, Ó., 2001. Holocene and pre-Holocene temporary disappearance of the George VI Ice Shelf, Antarctic Peninsula. *Antarct. Sci.* 13, 296–301.

- Holt, T.O., Glasser, N.F., Quincey, D., Siegfried, M.R., 2013. Speedup and fracturing of George VI Ice Shelf, Antarctic Peninsula. *Cryosphere* 7, 797–816.
- Hubbard, B., Glasser, N.F., 2005. *Field Techniques in Glaciology and Geomorphology*. Wiley.
- Hughes, P.D., Gibbard, P.L., Ehlers, J., 2013. Timing of glaciation during the last glacial cycle: evaluating the concept of a global 'Last Glacial Maximum' (LGM). *Earth-Science Rev.* 125, 171–198.
- Humbert, A., 2007. Numerical simulations of the ice flow dynamics of George VI Ice Shelf, Antarctica. *J. Glaciol.* 53, 659–664.
- Hunter, M.A., Riley, T.R., Cantrill, D.J., Flowerdew, M.J., Millar, I.L., 2006. A new stratigraphy for the Latady Basin, Antarctic Peninsula: Part 1, Ellsworth land volcanic group. *Geol. Mag.* 143, 777–796.
- Jamieson, S.S.R., Vieli, A., Ó Cofaigh, C., Stokes, C.R., Livingstone, S.J., Hillenbrand, C.-D., 2014. Understanding controls on rapid ice-stream retreat during the last deglaciation of Marguerite Bay, Antarctica, using a numerical model. *J. Geophys. Res.* 119, 1–17.
- Jamieson, S.S.R., Vieli, A., Livingstone, S.J., Ó Cofaigh, C., Stokes, C., Hillenbrand, C.-D., Dowdeswell, J.A., 2012. Ice-stream stability on a reverse bed slope. *Nat. Geosci.* 5, 799–802.
- Johnson, J.S., Everest, J.D., Leat, P.T., Gollidge, N.R., Rood, D.H., Stuart, F.M., 2012. The deglacial history of NW Alexander Island, Antarctica, from surface exposure dating. *Quat. Res.* 77, 273–280.
- Kilfeather, A.A., Ó Cofaigh, C., Lloyd, J.M., Dowdeswell, J.A., Xu, S., Moreton, S.G., 2011. Ice-stream retreat and ice-shelf history in Marguerite Trough, Antarctic Peninsula: sedimentological and foraminiferal signatures. *Geol. Soc. Am. Bull.* 123, 997–1015.
- King, M.A., Bingham, R.J., Moore, P., Whitehouse, P.L., Bentley, M.J., Milne, G.A., 2012. Lower satellite-gravimetry estimates of Antarctic sea-level contribution. *Nature* 491, 586–589.
- LaBarbera, C.H., MacAyeal, D.R., 2011. Traveling supraglacial lakes on George VI Ice Shelf, Antarctica. *Geophys. Res. Lett.* 38 (n/a–n/a).
- Laybourn-Parry, J., Quayle, W.C., Henshaw, T., Ruddell, A., Marchant, H.J., 2001. Life on the edge: the plankton and chemistry of Beaver Lake, an ultra-oligotrophic epishelf lake, Antarctica. *Freshw. Biol.* 46, 1205–1217.
- Leat, P., Scarrow, J., Millar, I., 1995. On the Antarctic Peninsula batholith. *Geol. Mag.* 132, 399–412.
- Lloyd Davies, M.T., Atkins, C.B., van der Meer, J.J.M., Barrett, P.J., Hicock, S.R., 2009. Evidence for cold-based glacial activity in the Allan Hills, Antarctica. *Quat. Sci. Rev.* 28, 3124–3137.
- Lucchitta, B.K., Rosanova, C.E., 1998. Retreat of northern margins of George VI and Wilkins ice shelves, Antarctic Peninsula. *Ann. Glaciol.* 27, 41–46.
- McCarron, J., Smellie, J.L., 1998. Tectonic implications of fore-arc magmatism and generation of high-magnesian andesites: Alexander Island, Antarctica. *J. Geol. Soc. Lond.* 155, 269–280.
- Morris, E., Mulvaney, R., 1996. Recent changes in surface elevation of the Antarctic Peninsula ice sheet. *Z. für Gletscherk. Glazialgeol.* 31, 7–15.
- Morris, E.M., 1999. Surface ablation rates on Moraine Corrie Glacier, Antarctica. *Glob. Planet. Change* 22, 221–231.
- Morris, E.M., Vaughan, A.P.M., 2003. Spatial and temporal variation of surface temperature on the Antarctic Peninsula and the limit of viability of ice shelves. In: Domack, E.W., Leventer, A., Burnett, A., Bindshadler, R., Conway, P., Kirby, M. (Eds.), *Antarctic Peninsula Climate Variability: Historical and Palaeoenvironmental Perspectives*, vol. 79. American Geophysical Union, Antarctic Research Series, Washington, D.C. pp. 61–68.
- Mulvaney, R., Abram, N.J., Hindmarsh, R.C.A., Arrowsmith, C., Fleet, L., Triest, J., Sime, L.C., Alemayehu, O., Ford, S., 2012. Recent Antarctic Peninsula warming relative to Holocene climate and ice-shelf history. *Nature* 489, 141–144.
- Ó Cofaigh, C., Davies, B.J., Livingstone, S.J., Smith, J.A., Johnson, J.S., Hocking, E.P., Hodgson, D.A., Anderson, J.B., Bentley, M.J., Canals, M., Domack, E., Dowdeswell, J.A., Evans, J., Glasser, N.F., Hillenbrand, C.-D., Larter, R.D., Roberts, S.J., Simms, A.R., 2014. Reconstruction of ice-sheet changes in the Antarctic Peninsula since the Last Glacial Maximum. *Quat. Sci. Rev.* 100, 87–110.
- Ó Cofaigh, C., Dowdeswell, J.A., Allen, C.S., Hiemstra, J.F., Pudsey, C.J., Evans, J., Evans, D.J.A., 2005a. Flow dynamics and till genesis associated with a marine-based Antarctic palaeo-ice stream. *Quat. Sci. Rev.* 24, 709–740.
- Ó Cofaigh, C., Larter, R.D., Dowdeswell, J.A., Hillenbrand, C.-D., Pudsey, C.J., Evans, J., Morris, P., 2005b. Flow of the West Antarctic Ice Sheet on the continental margin of the Bellingshausen Sea at the Last Glacial Maximum. *J. Geophys. Res.* 110, B11103.
- Pedley, M., Paren, J.G., Potter, J.R., 1988. Localised basal freezing within George VI Ice Shelf, Antarctica. *J. Glaciol.* 34, 71–77.
- Penkman, K.E.H., Preece, R.C., Keen, D.H., Maddy, D., Schreve, D.C., Collins, M.J., 2007. Testing the aminostratigraphy of fluvial archives: the evidence from intra-crystalline proteins within freshwater shells. *Quat. Sci. Rev.* 26, 2958–2969.
- Pope, P.G., Anderson, J.B., 1992. Late Quaternary glacial history of the northern Antarctic Peninsula's western continental shelf. In: Elliot, D.H. (Ed.), *Contributions to Antarctic Research III: Antarctic Research Series*, pp. 63–91.
- Powers, M.C., 1953. A new roundness scale for sedimentary particles. *J. Sediment. Petrology* 23, 117–119.
- Pritchard, H.D., Vaughan, D.G., 2007. Widespread acceleration of tidewater glaciers on the Antarctic Peninsula. *J. Geophys. Res.* 112, 01–10. F03S29.
- Pudsey, C.J., Evans, J., 2001. First survey of Antarctic sub-ice shelf sediments reveals Mid-Holocene ice shelf retreat. *Geology* 29, 787–790.
- Putkonen, J., Swanson, T., 2003. Accuracy of cosmogenic ages for moraines. *Quat. Res.* 59, 255–261.
- Rau, F., Braun, M., Saurer, H., Goßmann, H., Kothe, G., Weber, F., Ebel, M., Beppler, D., 2000. Monitoring multi-year snow cover dynamics on the Antarctic Peninsula using SAR imagery. *Polarforschung* 67, 27–40.
- Rebesco, M., Domack, E., Zgur, F., Lavoie, C., Leventer, A., Brachfeld, S., Willmott, V., Halverson, G., Truffer, M., Scambos, T., Smith, J., Pettit, E., 2014. Boundary condition of grounding lines prior to collapse, Larsen-B Ice Shelf, Antarctica. *Science* 345, 1354–1358.
- Reynolds, J.M., Hambrey, M.J., 1988. The structural glaciology of George VI Ice Shelf, Antarctic Peninsula. *Br. Antarct. Surv. Bull.* 79, 79–95.
- Riddle, M.J., Craven, M., Goldsworthy, P.M., Carsey, F., 2007. A diverse benthic assemblage 100 km from open water under the Amery Ice Shelf, Antarctica. *Paleoceanography* 22, 1–8. PA1204.
- Roberts, S.J., Hodgson, D.A., Bentley, M.J., Sanderson, D.C.W., Milne, G., Smith, J.A., Verleyen, E., Balbo, A., 2009. Holocene relative sea-level change and deglaciation on Alexander Island, Antarctic Peninsula, from elevated lake deltas. *Geomorphology* 112, 122–134.
- Roberts, S.J., Hodgson, D.A., Bentley, M.J., Smith, J.A., Millar, I.L., Olive, V., Sugden, D.E., 2008. The Holocene history of George VI Ice Shelf, Antarctic Peninsula from clast-provenance analysis of epishelf lake sediments. *Palaeogeogr. Palaeoclimatol. Palaeoecol.* 259, 258–283.
- Rydt, J.D., Gudmundsson, G.H., Corr, H., Christoffersen, P., 2013. Surface undulations of Antarctic ice streams tightly controlled by bedrock topography. *Cryosphere* 7, 407–417.
- Scambos, T., Fricker, H.A., Liu, C.-C., Bohlander, J., Fastook, J., Sargent, A., Massom, R., Wu, A.-M., 2009. Ice shelf disintegration by plate bending and hydro-fracture: satellite observations and model results of the 2008 Wilkins ice shelf break-ups. *Earth Planet. Sci. Lett.* 280, 51–60.
- Scambos, T., Hulbe, C., Fahnestock, M., 2003. Climate-induced ice shelf disintegration in the Antarctic Peninsula. In: Domack, E.W., Leventer, A., Burnett, A., Bindshadler, R., Conway, P., Kirby, M. (Eds.), *Antarctic Peninsula Climate Variability: Historical and Palaeoenvironmental Perspectives*, 79. American Geophysical Union, Antarctic Research Series, Washington, D.C. pp. 79–92.
- Scambos, T.A., Bohlander, J.A., Shuman, C.A., Skvarca, P., 2004. Glacier acceleration and thinning after ice shelf collapse in the Larsen B embayment, Antarctica. *Geophys. Res. Lett.* 31, L18402.
- Scambos, T.A., Haran, T.M., Fahnestock, M.A., Painter, T.H., Bohlander, J., 2007. MODIS-based Mosaic of Antarctica (MOA) data sets: continent-wide surface morphology and snow grain size. *Remote Sens. Environ.* 111, 242–257.
- Simkins, L.M., Simms, A.R., DeWitt, R., 2013. Relative sea-level history of Marguerite Bay, Antarctic Peninsula derived from optically stimulated luminescence-dated beach cobbles. *Quat. Sci. Rev.* 77, 141–155.
- Smellie, J.L., 2017. Antarctic Peninsula – geology and dynamic development. in press. In: Kleinschmidt, G. (Ed.), *Geology of the Antarctic Continent*. Gebrüder Borntraeger Verlagbuchhandlung, Stuttgart.
- Smith, A.M., Vaughan, D.G., Doake, C.S.M., Johnson, A.C., 1998. Surface lowering of the ice ramp at Rothera Point, Antarctic Peninsula, in response to regional climate change. *Ann. Glaciol.* 27, 113–118.
- Smith, C.G., 1987. The geology of parts of the west coast of Palmer Land. *Br. Antarct. Surv. Sci. Rep.* 112, 102.
- Smith, J.A., Bentley, M.J., Hodgson, D.A., Cook, A.J., 2007a. George VI Ice Shelf: past history, present behaviour and potential mechanisms for future collapse. *Antarct. Sci.* 19, 131–142.
- Smith, J.A., Bentley, M.J., Hodgson, D.A., Roberts, S.J., Leng, M.J., Lloyd, J.M., Barrett, M.S., Bryant, C.L., Sugden, D.E., 2007b. Oceanic and atmospheric forcing of early Holocene ice shelf retreat, George VI Ice Shelf, Antarctic Peninsula. *Quat. Sci. Rev.* 26, 500–516.
- Smith, J.A., Hodgson, D.A., Bentley, M.J., Verleyen, E., Leng, M.J., Roberts, S.J., 2006a. Limnology of two Antarctic epishelf lakes and their potential to record periods of ice shelf loss. *J. Paleolimnol.* 35, 373–394.
- Smith, J.A., Hodgson, D.A., Bentley, M.J., Verleyen, E., Leng, M.J., Roberts, S.J., 2006b. Limnology of two Antarctic epishelf lakes and their potential to record periods of ice shelf loss. *J. Paleolimnol.* 35, 373–394.
- Stone, J.O., 2000. Air pressure and cosmogenic isotope production. *J. Geophys. Res.* Solid Earth 105, 23753–23759.
- Sugden, D.E., Clapperton, C.M., 1980. West Antarctic Ice Sheet fluctuations in the Antarctic Peninsula area. *Nature* 286, 378–381.
- Sugden, D.E., Clapperton, C.M., 1981. An ice-shelf moraine, George VI Sound, Antarctica. *Ann. Glaciol.* 2, 135–141.
- Truffer, M., Echelmeyer, K.A., 2003. Of isbrae and ice streams. *Ann. Glaciol.* 36, 66–72.
- Turner, J., Lachlan-Cope, T.A., Marshall, G.J., Morris, E.M., Mulvaney, R., Winter, W., 2002. Spatial variability of Antarctic Peninsula net surface mass balance. *J. Geophys. Res.* Atmos. 107, AAC 4-1-AAC 4-18.
- Van Hove, P., Swadling, K.M., Gibson, J.A., Belzile, C., Vincent, W.F., 2001. Farthest north lake and fjord populations of calanoid copepods *Limnocalanus macrurus* and *Drepanopus bungei* in the Canadian high Arctic. *Polar Biol.* 24, 303–307.
- van Lipzig, N.P.M., King, J.C., Lachlan-Cope, T.A., van den Broeke, M.R., 2004. Precipitation, sublimation and snow drift in the Antarctic Peninsula region from a regional atmospheric model. *J. Geophys. Res.* 109, D24106.
- Vaughan, D., 2012. The ice sheet. In: Fox, A. (Ed.), *Antarctic Peninsula: a Visitor's Guide*. Natural History Museum, London, pp. 52–63.
- Veilleux, J., Mueller, D.R., Antoniadis, D., Vincent, W.F., 2008. Arctic epishelf lakes as sentinel ecosystems: past, present and future. *J. Geophys. Res.* Biogeosciences 113.

- Vincent, W.F., Laybourn-Parry, J., 2008. *Polar Lakes and Rivers: Limnology of Arctic and Antarctic Aquatic Ecosystems*. Oxford university press.
- Wasell, A., Håkansson, H., 1992. Diatom stratigraphy in a lake on Horseshoe Island, Antarctica: a marine-brackish-freshwater transition with comments on the systematics and ecology of the most common diatoms. *Diatom Res.* 7, 157–194.
- Whitehouse, P.L., Bentley, M.J., Le Brocq, A.M., 2012a. A deglacial model for Antarctica: geological constraints and glaciological modelling as a basis for a new model of Antarctic glacial isostatic adjustment. *Quat. Sci. Rev.* 32, 1–24.
- Whitehouse, P.L., Bentley, M.J., Milne, G.A., King, M.A., Thomas, I.D., 2012b. A new glacial isostatic adjustment model for Antarctica: calibrated and tested using observations of relative sea-level change and present-day uplift rates. *Geophys. J. Int.* 190, 1464–1482.